Sveriges lantbruksuniversitet
Swedish University of Agricultural Sciences

Department of Energy and Technology

Propensity of bed materials used in dual fluidized beds to retain ash-forming elements from biomass fuels

Björn Folkeson

Civilingenjörsprogrammet i energisystem

Examensarbete 2014:20
ISSN 1654-9392
Uppsala 2014

SLU, Swedish University of Agricultural Sciences
Faculty of Natural Resources and Agricultural Sciences
Department of Energy and Technology

Björn Folkeson

Propensity of bed materials used in dual fluidized beds to retain ash-forming elements from biomass fuels
Upptag av askämnen i bäddmaterial vid tvåbäddsförgasning av biobränslen

Supervisor: Placid Atongka Tchoffor, SP
Assistant examiner: Gunnar Larsson, Department of Energy and Technology, SLU
Examiner: Åke Nordberg, Department of Energy and Technology, SLU

EX0724, Degree Project in Energy Systems Engineering, 30 credits, Technology, Advanced level, A2E
Master Programme in Energy Systems Engineering (Civilingenjörsprogrammet i energisystem) 300 credits

Series title: Examensarbete (Institutionen för energi och teknik, SLU)
ISSN 1654-9392
2014:20

Uppsala 2014

Keywords: fluidized bed, ash retention, gasification, combustion, bed material

Online publication: http://stud.epsilon.slu.se

Abstract

The main aim of this work was to investigate the propensity of bed materials to retain ash-forming elements from biomass under conditions relevant to dual fluidized bed gasification (DFBG). The investigation was carried out in a laboratory-scale bubbling fluidized bed reactor in which biomass was gasified with steam and the unconverted char was combusted in the temperature range 800–900 ° C. Three bed materials (sand, olivine and bauxite) and two biomass fuels (forestry residue and wheat straw) were studied.

From the results obtained and literature on the ash transformation chemistry during thermal conversion of biomass, it was found that the extent to which ash-forming elements from biomass are retained on bed materials depend among other factors on (1) the abundance of ash-forming elements in the fuel, (2) the ability of the bed material to react and form compounds with ash-forming elements and (3) the atmosphere surrounding the fuel in the reactor. For example, Ca, P and K (which were among the most abundant ash-forming elements in the forestry residues) were also the main ash-forming elements retained on sand, olivine and bauxite during thermal conversion of the forestry residues. However, the retention of these elements differed on the three bed materials. With respect to reactor atmosphere, Ca and P were retained on olivine primarily during char combustion while the retention of K on olivine was somewhat similar during gasification and char combustion.

In addition to the experimental results, the effect of the retention of ash-forming elements on bed agglomeration tendency and the composition of the product gas is discussed as well as the relevance of the obtained results for the DFBG process.

Keywords: Fluidized bed, ash retention, gasification, combustion, bed material

Sammanfattning för beslutsfattare

I detta arbete studerades ansamlingen av askämnen på bäddmaterial vid förgasning och förbränning av biobränslen i fluidiserad bädd. Bäddmaterialen (kvarts-)sand, olivin och bauxit jämfördes både med avseende på benägenhet att ansamla askämnen och motstånd mot agglomerering. Dessutom undersöktes i vilken omfattning askämnen ansamlades på olivin under förgasning av skogsavfall i jämförelse med under förbränning av den kvarvarande koksen.

Resultaten visade att olivin var betydligt mer motståndskraftigt mot agglomerering än bauxit, som visade en motståndskraft mot agglomerering jämförbar med sandens. Det förväntades att sand skulle uppvisa lågt motstånd mot agglomerering på grund av högt innehåll av Si och påföljande bildning av kaliumsilikat med K från bränslet. Däremot var det oväntat att bauxit skulle uppvisa ett likartat lågt motstånd mot agglomerering trots att bäddmaterialet hade ett lågt innehåll av Si.

Under förgasning och förbränning av skogsavfall upptog olivin mindre Ca medan bauxit upptog mer P och sand upptog mer K från bränslet. I litteraturen föreslås att ett ökat upptag av vissa askännen kan påverka sammansättningen av produktgasen vid förgasning, men ingen skillnad kunde fastställas mellan bäddmaterialen i detta avseende. Om ett val mellan bäddmaterial skall göras för lämplighet i en industriell förgasningsprocess visar resultaten inte på någon betydande påverkan på gassammansättningen mellan bäddmaterialen, vilket föranleder slutsatsen att det billigaste bäddmaterialet med fördel kan användas så länge det tilltänkta bränslet är fritt från föroreningar och av lågt innehåll av ämnen som kan leda till agglomerering. Om ett mindre rent bränsle med högre innehåll av ämnen som kan leda till agglomerering ärt tänkt att användas, eller om det efterstävas en större säkerhet mot agglomerering i processen, är olivin fördelaktigt. Däremot finns flertalet andra faktorer som kan vara avgörande för ett bäddmaterials lämplighet, exempelvis inverkan på nedbrytning av tjära i produktgasen, som inte tas upp i detta arbete.

Populärvetenskaplig sammanfattning

I takt med att den atmosfäriska koncentrationen av koldioxid stiger och tillgången av fossila bränslen sjunker är alla lösningar välkomna som syftar till att minska beroendet av importerade fossila resurser och samtidigt inte bidrar till ökade utsläpp av växthusgaser. Energitekniker som omvandlar biobränslen till mer lättillgängliga energibärare möjliggör användning av energi utan nettobidrag till atmosfärens koldioxidkoncentration. Därför är det önskvärt att ersätta fossila bränslen i exempelvis transportsektorn med sådana som härrör från biomassa.

Det har visat sig svårt att omvandla all energi i biomassa på ett bra sätt: det är enkelt att exempelvis jäsa socker till etanol men svårare att få bakterier eller jästsvampar att bryta ned vedämne och andra komplicerade strukturer för att omvandla dem till flytande eller gasformiga energirika produkter. Det är problematiskt eftersom störst andel lättillgänglig energi i biomassa ofta finns i grödor som används till matproduktion, eller odlas på marker där mat kunde producerats. Biobränslen som inte konkurrerar med matproduktion, t.ex. med ursprung från skogsbruket, innehåller ofta större andel svårnedbrytbara strukturer. Processer som omvandlar dessa till energi är mycket eftertraktade. Det är relativt okomplicerat och mycket vanligt att exempelvis elda biomassa för att producera el och värme, och i framtiden är det sannolikt att stora delar av samhället kan vara eldrivet och hämta sin energi genom, bland annat, förbränning av biobränslen och från många andra förnybara källor. Men i väntan på att lagring av elenergi kan ske tillräckligt snabbt och i tillräckligt stora volymer behövs andra energibärare som ersätter fossila bränslen, i synnerhet inom transportsektorn. Att använda värme för att förgasa biomassa har samma fördelar som att elda dem och producera el, men med fördelen att energin i produktgasen relativt billigt kan lagras i stora kvantiteter och ”tankas” snabbt, i synnerhet om den syntetiseras till flytande bränsle.

Förgasning av biobränslen i två sammankopplade fluidiserade bäddar är en relativt ovanlig förgasningsteknik som har funnit tillämpning bland annat för att producera fordonsdrivmedel. Genom att under höga gashastigheter passera ånga genom vanlig sand eller något annat mineral – vilket i dessa tillämpningar kallas bäddmaterial – börjar bäddmaterialet bete sig som en bubblande vätska. När man introducerar en liten mängd bränsle i taget till bädden hettas bränslet snabbt upp och förgasas i den syrefria förgasningsreaktorn. Koksen, det vill säga det som återstår av bränslet när de mer lättillgängliga beståndsdelarna av bränslet förgasats, cirkuleras därefter tillsammans med bäddmaterialet till en förbränningsreaktor där luft tillsätts, vilket frigör värme när koksen brinner. Det varma bäddmaterialet cirkuleras därefter åter till förgasningsreaktorn och tillför därmed den värme som krävs för att förgasningsreaktionen skall ske. Fördelarna med tekniken är flera. Produktgasen hålls fri från avgaser från förbränningen och får därmed högt energiinnehåll, samtidigt som processen drivs utan tillskott av energi från andra källor än från det bränsle som förgasas. Den goda omblandningen i det fluidiserade bäddmaterialet gör att förgasningen kan ske vid låga temperaturer, vilket gör att utsläppen av kväveoxider hålls låga. Dessutom kan många askämnen med relativt låg smälttemperatur bevaras i fast form vilket förhindrar flera askrelaterade driftproblem. Att bränslet utgör en mycket liten del av den totala bäddmaterialets vikt gör att omvandlingen, till skillnad från konventionella förgasare, är okänslig för bränslets kvalitet både vad gäller innehåll av vatten och bränslets askhalt.

Asksammansättningen i bränslet spelar stor roll för processen. Ett högt innehåll av kalium i askan, till exempel, leder ofta till att legeringar av låg smältpunkt bildas om innehållet av kisel är högt i askan eller bäddmaterialet, vilket är fallet för vanlig sand. Detta kan göra så att bäddmaterialet klumpar sig – agglomererar – vilket kan leda till bäddkollaps och driftstopp. Därför är det viktigt att vara uppmärksam på hur bäddmaterialets sammansättning förhåller sig till bränsleaskans, framför allt vad gäller kalium, kisel,

natrium, fosfor, kalcium och magnesium. Vissa förhållanden mellan förekomsten av dessa ämnen i kombinationen av bäddmaterial och bränsle har visat sig öka risken för agglomerering. Genom att antingen ändra bränsle eller bäddmaterial kan man på så sätt styra processen i önskad riktning.

Alla askämnen ger däremot inte upphov till oönskade effekter. Till exempel motverkar flera askämnen agglomerering. Enligt vissa studier ökar nedbrytningen av tjära om kalium och klor avges från bränslet, vilket ökar kvaliteten av produktgasen. Andra försök har visat att tjärinnehållet i produktgasen minskar om järn finns i bäddmaterialet, eller att en katalytisk verkan på den s.k. vattengasskiftreaktionen erhålls om en beläggning av kalcium bildas på bäddmaterialet, vilket bildar mer koldioxid och vätgas vid förgasning i ånga. I samtliga fall är det relevant att veta i vilken omfattning olika askämnen binder till olika bäddmaterial för att kunna förutse driftproblem eller kunna dra nytta av askkemin.

För att undersöka hur askämnen ansamlas på bäddmaterial och hur de i sin tur påverkar gasutbytet genomfördes en serie labbförsök. Två biobränslen, skogsavfall i form av grenar och toppar samt vetehalm, maldes och pelleterades. Bäddmaterialen sand, bauxit och olivin användes: alla tre är naturligt förekommande bergarter men har olika sammansättning och egenskaper som är av intresse för processen. Sand är rikt på kisel vilket kan leda till agglomereringsproblem, medan både olivin och bauxit tidigare har visats vara motståndskraftiga mot agglomerering. I försöken med vetehalm visade det sig att olivin hade större motståndskraft mot agglomerering än bauxit, som i sin tur hade ungefär samma motståndskraft mot agglomerering som sand. Resultatet var i enlighet med litteraturen vad gällde olivin och sand, men den låga motståndskraften hos bauxit var oväntad.

I den serie försök där samma mängd skogsavfall matades till reaktorn framgick tydliga skillnader mellan bäddmaterialen angående i vilken omfattning askämnen ansamlades på bäddmaterialens yta. I samtliga fall dominerade upptaget av kalcium, fosfor och kalium. Olivin upptog däremot mindre kalcium än de andra bäddmaterialen, medan bauxit upptog mer fosfor och sand upptog mer kalium. I samma försök mättes sammansättningen av produktgasen. Sett till enbart sammansättningen av de enskilda gaserna var skillnaderna små mellan de olika bäddmaterialen. Däremot visade det sig att koncentrationen av kolmonoxid och metan sjönk allt eftersom försöket pågick, medan koncentrationen av koldioxid steg. Detta kan tydas som en successivt ökad katalys av vattengasskiftreaktionen under försöket, möjligen härrörande från askämnen.

I ett försök på olivin provtogs bäddmaterialet på ett sätt som gjorde det möjligt att utröna i vilket skede de olika askämnena ansamlades på bäddmaterialet. Både kalcium och fosfor upptogs på bäddmaterialet i störst omfattning under förbränningssteget, medan kalium upptogs både under förbrännings- och förgasningssteget. Skälet är troligtvis att kalcium och fosfor bildar föreningar som inte avgår från bädden under de aktuella temperaturerna, medan kalium är mer lättflyktigt och därför kunde både avgå från bränslet och ansamlas på bäddmaterialet under båda stegen.

Med stöd av resultaten kan en jämförelse göras mellan bäddmaterialens lämplighet. Eftersom skillnaden var liten mellan bäddmaterialen vad gäller inverkan på gassammansättningen kan det billigaste av dem med fördel användas i tillämpningar där bränslet är fritt från föroreningar och av låg halt av askämnen som smälter vid låg temperatur. Om bränslet däremot innehåller en viss andel föroreningar eller askämnen som medför risk för agglomerering finns anledning att använda olivin i processen. Eftersom olivin visade sig ha betydligt större motståndskraft mot agglomerering medför dess användning att risken för oplanerade driftstopp blir lägre, vilket även kan möjliggöra att bränslen av något lägre eller skiftande kvalitet kan användas i processen. Detta måste däremot vägas mot en rad andra faktorer, däribland en högre bäddmaterialkostnad.

Preface

I would like to thank all the colleagues at SP Technical Research Institute of Sweden who I have come in contact with during the work with this thesis, as I have received kind help with everything ranging from practical problems in the lab to theoretical inquiries. I would like to extend additional gratitude to the following persons:

- Kent Davidsson for valuable discussions and input
- Daniel Ryde for frequent help and company in the lab
- Gunnar Larsson of the Swedish University of Agricultural Sciences for reviewing and commenting this report
- Nijaz Smajovic and Mathias Berglund of SP Chemistry for loan of equipment and for kind patience during my lab visits

Last but not least, I would like to thank my tutor Placid Atongka Tchoffor for all the time and effort invested in explaining concepts, co-conducting experiments and analyses, reviewing this report and providing guidance all throughout the process of the production of this work.

Table of Contents

Nomenclature

Al	Aluminium (chemical element)
Ba	Barium (chemical element)
BFB	Bubbling fluidized bed
Ca	Calcium (chemical element)
CFB	Circulating fluidized bed
Cl	Chlorine (chemical element)
DFB	Dual fluidized bed
DFBG	Dual fluidized bed gasification
FB	Fluidized bed
FBC	Fluidized bed combustion
FBG	Fluidized bed gasification
Fe	Iron (chemical element)
K	Potassium (chemical element)
LHV	Lower heating value
Mg	Magnesium (chemical element)
Mn	Manganese (chemical element)
Na	Sodium (chemical element)
NDIR	Nondispersive infrared
P	Phosphorus (chemical element)
S	Sulfur (chemical element)
SEM-EDX	Scanning electron microscopy with energy-dispersive x-ray spectroscopy
Si	Silica (chemical element)
SMD	Sauter mean diameter
Ti	Titanium (chemical element)
XRD	X-ray diffraction
XRF	X-ray fluorescence

Symbols in mathematical expressions

μ	Absolute or dynamic viscosity [N s/m^2]
μ_{cg}	Cold gas efficiency [-]
ρ_g	Gas density [kg/m^3]
ρ_p	Bed material particle density [kg/m^3]
Ar	Archimedes number [-]
d_i	Mean aperture size [µm]
d_p	Mean particle diameter [µm]
$\dot{m}_{fuel}$	Mass flow rate of fuel [kg/h]
$\dot{m}_{gas}$	Mass flow rate of product gas from a gasifier [kg/s]
Q_{fuel}	Lower heating value of fuel [MJ/kg]
Q_{gas}	Lower heating value of product gas from a gasifier [MJ/kg]
R	Molar gas constant [J/kmol]
Re_{mf}	Reynolds number at minimum fluidization velocity [-]
T	Temperature [K]
U_t	Terminal velocity [m/s]
U_{mf}	Minimum fluidization velocity [m/s]
x_i	Mass fraction [-]

1 Introduction

1.1 Background

In line with increasing concern of diminishing fossil energy resources, rising atmospheric concentration of carbon dioxide and global mean temperature levels, much scientific effort has been focused on optimizing the use of renewable and carbon-neutral biomass for energy production. One of the more promising technologies that can be applied to produce readily available and storable energy from biomass is *dual fluidized bed gasification* (DFBG). In this process, which is carried out in two interconnected fluidized beds (FB), biomass is gasified to produce an energy-rich gas of energy content 10–18 MJ/Nm^3 (Basu, 2006). The DFBG technology advantage over other types of gasifiers is mainly due to the ability to prevent nitrogen dilution of the product gas while simultaneously conducting the process without the need of addition of external heat. The gas can be directly combusted in a gas turbine to produce electricity and heat, or upgraded to biomethane and used as a transportation fuel or as a raw material in the synthesis of other fuels and high-value chemicals. Some biomass fuels that can be readily used in this process are wood and bark, and with proper care fuels such as forestry residues (occasionally denoted by the Swedish term *grot*) and straw can be used.

Although not widespread, DFBG processes have been demonstrated to function in smaller scale for some years. A fast internally circulating fluidized bed gasifier in Güssing, Austria has been in operation since 2001 and converts biomass fuel at a fuel input rate of 8 MW in a steam-blown dual fluidized bed gasifier (Rauch et al., 2004, Ahrenfeldt et al., 2013). The Güssing system has a cold gas efficiency[1] of 55–60 % while a commercial DFBG project in Gothenburg, Sweden is projected to produce 100 MW of biomethane from biomass at a cold gas efficiency of 65 %. Research into higher efficiencies is underway: a laboratory-scale circulating FB reactor at the Technical University of Denmark has achieved a cold gas efficiency around 90 % (Ahrenfeldt et al., 2013).

One key aspect in improving cold gas efficiency as well as the lifetime and performance reliability of a plant for gasification or combustion of biomass in fluidized bed is the transformation of ash-forming elements in biomass fuels. While giving rise to several undesired effects such as agglomeration of bed material, corrosion and fouling of heat transferring surfaces, some of the effects of ash transformation are beneficial. During fluidized bed gasification, certain ash-forming elements that interact with bed material have been shown to reduce tars in the product gas. Other combinations of ash elements and bed material display a catalytic effect on the water gas-shift reaction, thereby increasing the hydrogen content in the product gas.

Ash retention in the bed material is also the principle cause of sintering and agglomeration in the context of FB processes, on which much work has been focused (Skrifvars et al., 1994). The rate of agglomeration observed in the bed differs across bed materials. For example the presence of aluminium in e.g. bauxite inhibits sintering, while it has been shown that defluidization times (the time taken for a fluidized bed to collapse when continuously fed) are greatly prolonged if bauxite rather than silica sand is used as bed material when combusting coal. This suggests the use of bauxite might be strongly favorable in this regard (Vuthaluru et al., 1999, Kuo et al., 2008) In a similar manner, the use of olivine as bed material has been shown to increase the temperature at which defluidization occurs, as well as acting as a catalyst of tar cracking when gasifying fuels (Fryda et al., 2008, Mastellone and Arena, 2008).

During DFBG or any other energy application of fluidized beds, it is of interest to avoid or to mitigate the negative effects of ash interaction with the bed material while taking benefit from its positive effects. In order to accomplish this, attention needs to be directed toward selecting the right combination of fuel and bed material. This choice can only be made if it is known how the ash-forming elements interact with the bed material.

[1]A relationship between the energy content of the product gas and the fuel energy input. For details, see Section 2.3.1.

Ash deposition on the bed material is central for agglomeration behavior as well as for catalytic effects. Decisive factors that are crucial to manage well in any FB application for gasification or combustion include the mechanism with which ash elements interact with the bed material, which chemical form they take, which ash elements that are present in the fuel and the rate at which ash elements accumulate on the bed material. Yet, the tendency of bed materials to capture and retain ash elements is only partially reviewed in literature even though the underlying principles of the individual processes of sintering and agglomeration are well understood. In the context of ash retention on bed material, previous studies have more often focused on macro effects of ash retention, such as agglomeration. Fewer studies have focused on the ash retention itself, and fewer still have systematically compared different bed materials in this aspect. In addition, the papers on bed agglomeration have, to a large extent, been separated from those on catalytic effects owing to ash retention in the bed material. Since the retention of ash elements in the bed material is central to both phenomena, this work will be carried out with both in mind.

If the processes of ash retention on bed material can be better understood, operational and economic benefits may be an outcome due to better knowledge of how to control thermal processes in fluidized beds. The results of this study should therefore be of value to the industries seeking to further understand the properties and behavior of biomass fuel and bed material in fluidized bed gasification and combustion.

1.1.1 Aim

The purpose of this thesis was to investigate the tendency of bed materials to retain ash-forming elements from biomass under conditions relevant to dual fluidized bed gasification. In addition, the influence of this retention with respect to product gas composition and the resistance of the bed materials to be agglomerated was investigated.

The results obtained will provide knowledge on ash retention on bed materials during thermal conversion of biomass that can be used to enhance the beneficial effects of ash retention while avoiding or mitigating its disadvantages. From this, conclusions may be drawn which can be of use in the design and operation of fluidized bed reactors as well as for selecting a suitable bed material for a DFBG process with respect to agglomeration tendency and influence on gas composition.

1.1.2 Scope

Each industrial process for combustion and gasification in fluidized beds has different aims and operating parameters. For instance, gas yields and decomposition of tars can be controlled through managing the reaction temperature. Since the parameters are different for each application it is difficult to draw general conclusions about whether or not the ash chemistry of a fuel or bed material is beneficial for all processes. For this reason, the scope of this work is limited to the retention of ash-forming elements for different combinations of fuels and bed materials under a single set of parameters. Aspects such as temperature dependency are not discussed. The application and relevance of results to specific processes are left to the reader.

In order to compare the extent of the accumulation of ash-forming elements on the bed material across different fuels it might be useful to include a commonly used fuel, e.g. wood pellets, for reference. However, due to the low ash content in the fuel and low content of elements prone to react with the bed material, wood pellets was not included in this study. In order to achieve sufficiently high amounts of retained ash on the bed materials for analysis, an experiment of a longer run time would have been required. For this reason, wood pellets was not studied.

This work is limited to surface analysis of virgin and used bed materials (carried out with *x-ray fluorescence* (XRF)). As such, standard chemical analysis of the samples to determine total weight concentration of elements or analysis to determine the chemical form of elements was not undertaken.

2 Literature review

In the following sections, relevant topics and concepts are presented. Sources include reference literature for formulae and constants as well as textbooks covering technical aspects of fluidized bed gasification and combustion. The bulk of the material, however, is based on published journal articles on the topics. The literature review covers biomass fuel and its composition, fluidization principles and descriptions of fluidized bed reactors, the role of bed materials in the processes as well as theory concerning thermal conversion of fuel. Finally, the influence of ash elements on fluidized bed gasification and combustion processes are presented.

2.1 Biomass fuels

In every instant, solar radiation passes through the atmosphere and strikes the surface of the earth with a constant power in the range of 10^{17} W, accounting for a yearly insolation of roughly 3 000 000 EJ (Jenkins et al., 1998). A fraction of this irradiation strikes chlorophyll pigments in photosynthesizing organisms and is put to use in building carbohydrates with water and carbon dioxide as feedstocks. As such, the sun is the driving force in the production of what is referred to as biomass. In this definition are not only all plants included, seeing that they are composed of matter built through photosynthesis, but also as all organisms that nurture themselves on those that photosynthesize. Matter originating from organisms is included as well: animal wastes and discarded leaves are examples of this. In a wider sense, one could define biomass as all matter that constitutes or originates from organisms which draw their energy from the sun, or from consuming organisms that do. In terms of biological global production of biomass, some 1 000 EJ is produced annually (Jenkins et al., 1998). As a comparison, the world primary energy consumption in the year of 2012 was just under 200 EJ (BP, 2013).

2.1.1 Biomass composition

The composition of biomass differs significantly for different fuels. Since the composition of biomass influences many of the properties exhibited by the fuel during thermal conversion, methods for determining biomass composition are presented in the following sections. An illustration of the composition of biomass is presented in Figure 2-1.

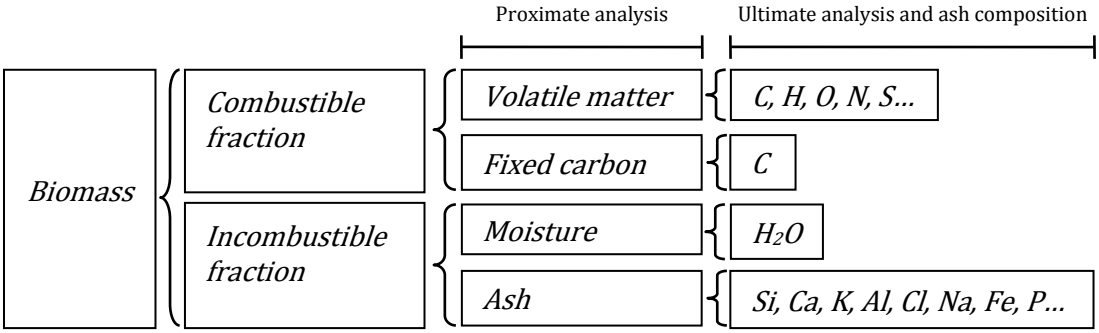

Figure 2-1. Composition of biomass in a simplified illustration.

2.1.1.1 Structural composition

In determining the heating value of a biomass fuel it is of interest to evaluate its structural composition. Plant tissue, created through photosynthesis, consists of carbohydrates in various forms. The main constituents are cellulose, hemicellulose and lignin but other important components include simple sugars, starches, lipids, proteins and hydrocarbons (Jenkins et al., 1998).

2.1.1.2 Ultimate composition

In determining combustion and gasification properties, such as to what extent a given biomass fuel would give rise to emissions such as SO_x and NO_x, the *ultimate composition* is of importance. This analysis states the composition of the fuel in terms of its basic elements: often C, H, N, O and S (Basu, 2010). Owing to the carbohydrate structure, biomass has a high content of oxygen, which commonly makes up around 30–40 % of the dry mass (Jenkins et al., 1998). Compared to bituminous or lignite coal which has an oxygen content (which does not contribute to the energy content) in the range of

10–20 %, this factor helps explain why coal is of higher energy content than biomass (McKendry, 2002, Basu, 2010).

2.1.1.3 Proximate composition

In order to determine the behavior of biomass fuel under thermal conversion a *proximate analysis* is undertaken, which is indicative of heating value as well as expected tar yield and ash problems. A proximate analysis presents the fuel composition in terms of its principal components: moisture, volatile matter, fixed carbon and ash content.

The compounds that burn, gasify or volatilize when subject to heating form the *combustible fraction* of the fuel where the *volatile matter* and the *fixed carbon content* of the fuel are parts (Jenkins et al., 1998). Volatile matter is defined as the fuel constituents which volatilize and leave the fuel matrix as vapors when pre-dried biomass is heated according to set standards, commonly to around 900 °C (Basu, 2010). Biomass is usually high in volatile matter: a content in the region of 80 % is not uncommon, which can be compared to that of bituminous or lignite coals which have a volatile matter content of approximately 30 % (McKendry, 2002).

The fixed carbon content is the combustible fraction of the fuel that is not volatilized upon heating. After measuring the moisture content, the ash content and the volatile matter content, the fixed carbon content is measured indirectly by subtracting these components from the initial fuel sample weight Together with the fuel ash, the fixed carbon of the fuel forms char in the process of devolatilization (Basu, 2010).

The ash content, together with the moisture content, forms the incombustible fraction of the fuel. The ash content is the solid residue left after complete combustion (Basu, 2010). In the ideal ash, no combustible elements remain. In essence, the ash can be thought of as the concentrate of the incombustible and inorganic elements which are dispersed in the fresh fuel. However, the ash constituents are not fully representative of the original inorganic fuel constituents as the inorganic ash elements in the ash are found in oxidized forms, which is not necessarily the case in the fresh biomass (Jenkins et al., 1998, Basu, 2010). In addition, certain ash elements are prone to volatilize in the gasification or combustion process.

Although the mentioned components are those that constitute all biomass, their relative proportions vary significantly across biomass fuels. This variation is important in the context of gasification and combustion properties. For instance, a high ash content when compared to woody biomass is typical of fast-growing crops and agricultural biomass fuels: wheat straw may contain 11 times as much ash as wood pellets as illustrated in Figure 2-2.

The volatile matter content and fixed carbon content also differ between species. In Figure 2-2, the diverse nature of biomass composition is presented in terms of the dry basis content of fixed carbon, volatile matter and ash for a few example fuels.

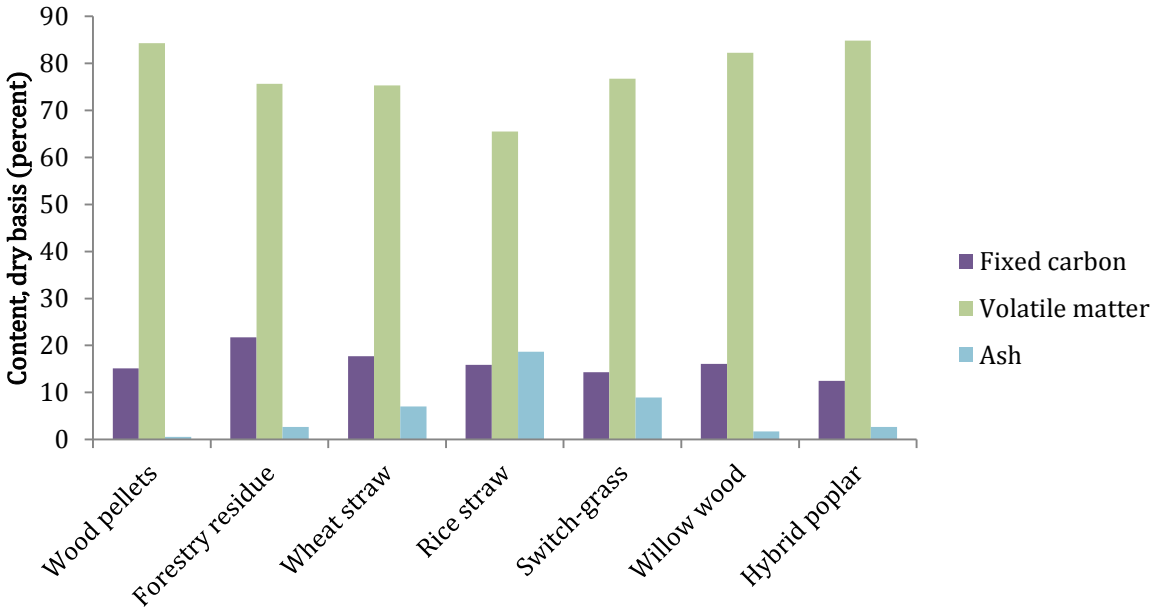

Figure 2-2. Typical content of ash, volatile matter and fixed carbon in selected biomass species. Data from multiple sources (Jenkins et al., 1998, Strömberg and Svärd, 2012).

The proximate composition of the fuel varies depending on which section of the plant is used. For example, stemwood has a lower ash content than bark, which typically has a lower ash content than the needles or foliage of a tree (Werkelin et al., 2005). This means that storage influences the proximate composition as well: for example, the ash content for coniferous biomass generally decreases with storage time through the process of defoliation (Lehtikangas, 1998). In addition, the proximate composition is also dependent on handling and harvesting methods and what stage of growth the plant was in at the time of harvest (Jenkins et al., 1998).

2.1.1.3.1 Ash composition

Since the focus of this work is on the retention of ash-forming elements on the bed material, it is of importance to look at the composition of the biomass ash in detail. In fact, the presence of ash-forming elements are highly decisive for the performance, life time and efficiency of a thermal conversion plant. Therefore not only the ash content but also the ash composition of a biomass fuel is essential, which is included in a detailed proximate analysis.

The main ash-forming elements in biomass fuels are Si, K, Na, Al, Fe, P, S, Cl, Mn, Ca and Mg (Basu, 2010, Saidur et al., 2011). In addition, several trace elements can be found in biomass ash. The concentrations of these elements vary from one biomass type to another. Woody biomass ash is typically high in Ca and low in Si. Agricultural crops in general are usually rich in Si while straws and cereals in particular are rich in K and Cl (Saidur et al., 2011). For example, the potassium concentration in wheat straw is 2 to 3 times higher and its Si content is 2 to 23 times higher than in ashes of woody biomass. This is illustrated in Figure 2-3, where element concentrations in ash are presented for common biomass fuels. The data was mainly taken from literature presenting the occurrence of the chemical compounds that constitute the ash, and have hence been recalculated to reflect the elemental composition. In many gasification and combustion applications, the properties of wood pellets are used as a benchmark. In order and to assist in comparison of fuels, data on element concentrations in common biomass ash is therefore presented in a normalized form with wood pellets as basis in Figure 2-3.

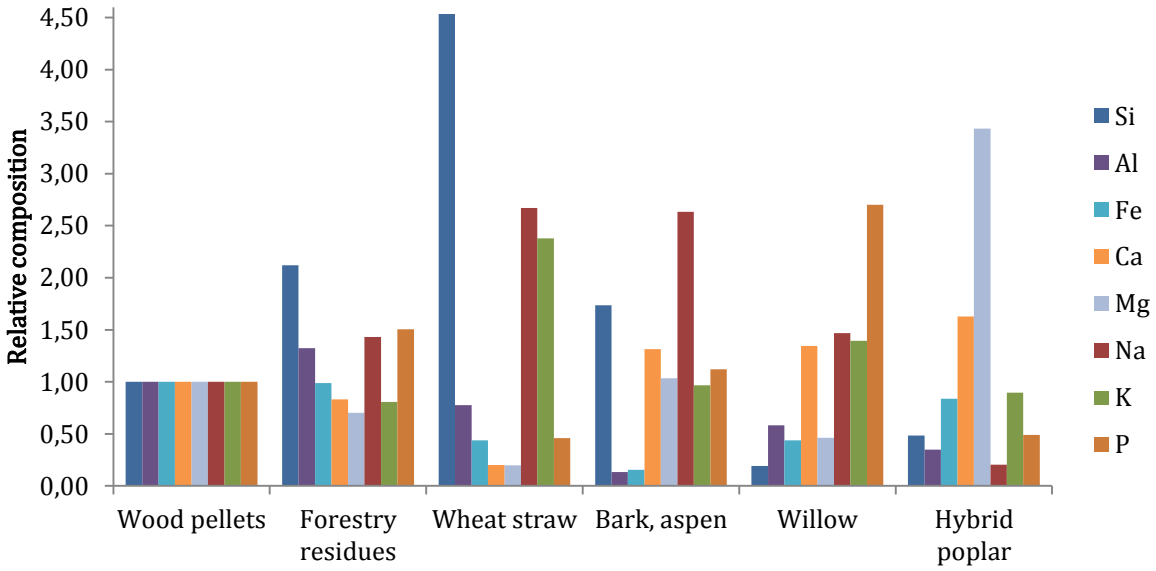

Figure 2-3. Normalized concentrations of elements in ash of common biomass fuels. Basis for normalization is wood pellets. Data from multiple sources (Strömberg and Svärd, 2012, Jenkins et al., 1998).

It should be noted that harvesting, storage and handling methods influence ash content and ash composition and consequently the combustion and gasification behavior of a biomass fuel. Biomass subject to extensive handling and harvesting processes, such as forestry residues, may collect dirt or other incombustible substances during these processes. This increases the ash content of the fuel and influences the ash composition toward higher content of Si (Lehtikangas, 1998). This is shown in Figure 2-3. In the case of wheat straw, storage methods influence the alkali content. Exposure to precipitation has been shown to reduce the wheat straw's content of water soluble ash elements, notably K and Cl, through leaching (Strömberg and Svärd, 2012). One study concluded, in accordance with other literature, that over 80 % of the K present in wheat straw was easily soluble in water (Tchoffor et al., 2013).

2.2 Fluidized beds

In the following sections, the theory describing the fundamental principles of operation of fluidized beds for are summarized.

2.2.1 Fluidization principles

Fluidized beds utilize a gas stream to suspend particles in the reactor vessel. This causes the collection of particles to behave much like a fluid both in the sense that it conforms to the container walls and that the surface of the fluidized bed remains flat, were the container to be tilted (Alvarez, 2006).

In contrast to thermal conversion of biomass in fixed beds, thermal conversion of biomass in fluidized beds takes place with an inert material present in the bed. This inert material, commonly called *bed material*, serves the purpose of transferring heat to the fuel particles in the reactor. In this sense, the bed material can be said to act as a thermal buffer. Typically, less than 10 percent of the total bed weight is comprised of fuel particles while the inert bed material represents the bulk of the weight (Alvarez, 2006).

2.2.1.1 Minimum fluidization velocity

In a given system, the *minimum fluidization velocity* U_{mf} describes the minimum velocity of the fluidization medium at which the bed is fluidized. At minimum fluidization velocity, the bed material can be said to undergo a phase change.

This behavior can be visualized if the pressure drop over the bed Δp is plotted against superficial gas velocity U_{mf}, creating a *fluidization plot*. As the gas velocity is increased, the pressure drop increases

at a lower rate or ceases to increase. The intersection between the lines describing the pressure drop over the bed in the non-fluidized versus the fluidized state defines the *minimum fluidization velocity* which can be read on the velocity axis. This is illustrated in a simplified manner in Figure 2-4. However, the transition to and from a fluidized state might not be well pronounced and subject to hysteresis (Ojha et al., 2000).

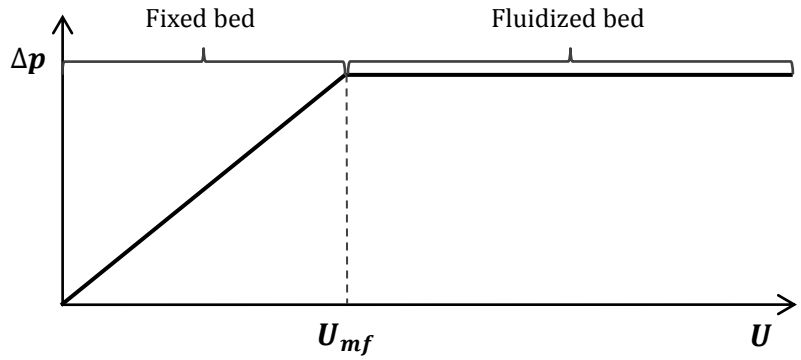

Figure 2-4. Simplified illustration of minimum fluidization velocity.

In the context of fluidized beds, the minimum fluidization velocity is denoted U_{mf} and can be expressed as (Basu, 2006):

$$U_{mf} = \frac{Re_{mf}\mu}{d_p\rho_g}. \tag{2.1}$$

Here, Re_{mf} denotes the Reynolds number when the bed has reached minimum fluidization and μ denotes the absolute or dynamic viscosity of the fluidizing medium, while d_p and $\rho_g$denotes the mean particle diameter and density of the bed material, respectively (Basu, 2006).

The expression for minimum fluidization velocity can be combined with the simplified expression of Re_{mf} (Basu, 2006):

$$Re_{mf} = [C_1 + C_2 Ar]^{0.5} - C_1. \tag{2.2}$$

The constants C_1 and C_2 are determined experimentally, and several suggestions of their value have been reported in literature. The different values suggested are based on different sets of experimental data for correlation (Yang, 2003). For fine particles the fit to experimental data has been shown to be best using values 27.2 for C_1 and 0.0408 for C_2 and these values have been chosen for this work (Grace, 1982). Ar denotes the Archimedes number which in turn can be expressed as:

$$Ar = \frac{\rho_g(\rho_p - \rho_g)g d_p^3}{\mu^2}. \tag{2.3}$$

Combined, (2.1, (2.2 and (2.3 can be used to express the minimum fluidization velocity. If the minimum velocity is multiplied with the bed cross sectional area as in (2.8, the corresponding volume flow may be obtained.

If not taken from literature, the absolute or dynamic viscosity μ for a certain temperature can be calculated for a given temperature using Sutherland's equation (Sutherland, 1893):

$$\mu = \mu_{ref} \left(\frac{T}{T_{ref}} \right)^{3/2} \frac{T_{ref} + S}{T + S}. \tag{2.4}$$

Here, μ_{ref} is used to denote the absolute or dynamic viscosity of the gas at the reference temperature T_{ref} (Sutherland, 1893), T denotes the temperature for which μ is sought while S denotes Sutherland's coefficient for the gas (Sutherland, 1893).

2.2.1.2 Terminal velocity

In a FB reactor the minimum fluidization velocity describes the velocity at which the system undergoes transition to a fluidized phase. In a similar fashion, the *terminal velocity* U_t describes the gas velocity at which the fluidized particles start to be transported out of the reactor along with the fluidizing medium. The term originates from the description of a freefalling particle in a homogeneous and stationary medium. It describes the velocity the freefalling particle reaches once the fluid drag and buoyancy forces acting on it reaches equilibrium with the forces of gravitation (Basu, 2006). In fluidization contexts, the terminal velocity describes the maximum superficial velocity of the fluidization medium where the particles forming the bed remain stationary, in average, as observed from a fixed external reference system.

The superficial velocity where this occurs can be described by three laws, each valid for a specific region of Reynolds number and only for spherical particles: for a more accurate estimation of terminal velocity the sphericity of the particles should be corrected for (Basu, 2006).

Stokes' law is valid at lower Reynolds numbers (Basu, 2006):

$$\frac{d_p U_t \rho_g}{\mu} = \frac{Ar}{18} \qquad Re < 0.4. \tag{2.5}$$

For the intermediate region of Reynolds numbers, the intermediate law applies (Basu, 2006):

$$\frac{d_p U_t \rho_g}{\mu} = \left(\frac{Ar}{7.5} \right)^{0.666} \qquad 0.4 < Re < 500. \tag{2.6}$$

At higher Reynolds numbers, Newton's law is valid (Basu, 2006):

$$\frac{d_p U_t \rho_g}{\mu} = \left(\frac{Ar}{0.33} \right)^{0.5} \qquad Re > 500. \tag{2.7}$$

2.2.1.3 Superficial gas velocity

Minimum fluidization velocity and terminal velocity is expressed in terms of *superficial velocity* U, which in this context is defined as the gas volume flow Q through a cross section of the bed A (Basu, 2006):

$$U = \frac{Q}{A}. \tag{2.8}$$

In this work superficial velocity is occasionally referred to as the *velocity*.

2.2.2 Particle classification

The particle size distribution is an essential parameter for understanding both chemical and physical aspects of fluidized beds. It is a decisive factor in determining U_{mf} and U_t and influences reaction rates involving the bed material as well. A smaller particle size yields significantly lower artificial velocities for U_{mf} and U_t and increases reaction rates due to a higher surface to volume ratio. Since this ratio determines several aspects of bed material behavior, the surface to volume ratio is the basis

for expression of particle size distribution in calculations concerning fluidized bed systems. The surface-volume mean diameter, or *Sauter mean diameter* (SMD), is defined as the diameter of an equivalent sphere which has a surface to volume ratio equal to the actual particle population (Basu, 2006). Empirically, it is determined through sieve analysis where the sample is passed through a stack of sieves with decreasing aperture size. The weight retained on each sieve after a period of agitation is divided by the total sample weight to obtain the weight fraction x_i. The weight fraction is divided by d_i, the mean value of the aperture sizes of the sieve the material is retained on and the sieve through which it has passed. When inverted, this sum describes the SMD according to (2.9 (Basu, 2006):

$$SMD = \frac{1}{\sum\left(\frac{x_i}{d_i}\right)}. \tag{2.9}$$

2.2.2.1 Geldart classification

Different types of particles behave in a highly dissimilar fashion when subject to the fluidization medium. Some particle species fluidize easily with bubbles appearing close to U_{mf} while others are hard to fluidize at all. For the highest accuracy, the specific fluidization properties of every particle type needs to be empirically determined prior to selecting the bed material for a FB process.

In order to circumvent this need, Geldart developed a characterization of powders into four distinguishable groups based on the mean particle size of the particles and their density difference in relation to the fluidization medium (Geldart, 1973). The properties of the particles within the group can be considered to correlate reasonably well within the group, which is of great use in predicting the properties of a given particle type using only simple metrics (Geldart, 1973).

Determining the Geldart group of a particle type is done through reading the corresponding regions in the Geldart diagram, where mean particle size is plotted against density difference of particles and fluidization medium. Properties of particles in the four Geldart groups are presented in Table 2-1.

Table 2-1. Geldart classification of particle species. Data from multiple sources (Geldart, 1973, Basu, 2006).

	Geldart group A	Geldart group B	Geldart group C	Geldart group D
Mean particle size d ($\rho_p = 2\,500$ kg/m³) [μm]	20 < d < 90	90 < d < 650	d < 20	d > 650
Special characteristics	Small, light particles	Sand-like particles	Cohesive particles	Large, dense particles
Velocity for fluidization	Low	Medium	Difficult to fluidize (channeling)	High
Expansion of bed	Considerable	Some	None	Some
Mixing in incipient fluidization	Good	Some	None	Poor
Velocity when bubbles appear (bubble point)	Higher than minimum fluidization velocity	Close to minimum fluidization velocity	No bubbles	Close to minimum fluidization velocity
Bubble velocity relative interstitial gas velocity	Faster	Slightly faster	No bubbles	Slower
Maximum bubble size	Yes	No	No bubbles	-

2.2.3 Fluidization states

The velocity of the gas coming into contact with the bed defines the type of FB system. An air velocity insufficient to break the cohesive forces of the bed material is characteristic of conventional grate combustion, where primary air is injected below the fuel bed. As the gas velocity is increased, the gas increasingly interacts with the bed material through frictional forces to weaken the cohesion of the fuel bed while simultaneously counteracting the gravitational pull on the fuel bed. In this fixed-bed phase, ranging from no to partial (or incipient) fluidization, the pressure drop over the bed is proportional to the gas velocity.

At speeds at or over minimum fluidization velocity, turbulence in the bed creates a pronounced stirring causing the fuel and bed material particles to be exposed to the gas stream uniformly. As the space between the particles increases, so does the apparent volume of the fluidized bed. The pressure drop over the bed in this phase is no longer proportional to the gas velocity, as is the case when a fixed bed is concerned. A higher gas velocity yields a proportionally smaller increase in pressure drop over the bed compared to the non-fluidized or partially fluidized state (Alvarez, 2006). Observations of the pressure drop over the bed can therefore be employed to determine its fluidization state.

As the fluidization velocity is varied, different types of fluidization states can be distinguished, each with defining characteristics. In Table 2-2, which applies to Geldart type B particles, bed fluidization states are presented along with associated typical velocities of the gasifying medium and examples of their application. In Figure 2-5, these fluidization states are illustrated.

Table 2-2. States of fluidization, typical gas velocities and applications. Modified from original source (Basu, 2006).

	Fixed bed	**Incipiently fluidized bed**	**Bubbling fluidized bed**	**Turbulent fluidized bed**	**Fast fluidized bed**	**Pneumatic transport**
Gas velocity	→					
	$0 \leq U_{mf}$	$= U_{mf}$	$\geq U_{mf}$			$\gg U_{mf}$
	e.g. 0–3 m/s	e.g. 0.5–2.5 m/s			e.g. 4–6 m/s	e.g. 15–30 m/s
Application	Grate firing	BFB			CFB	Pulverized coal firing

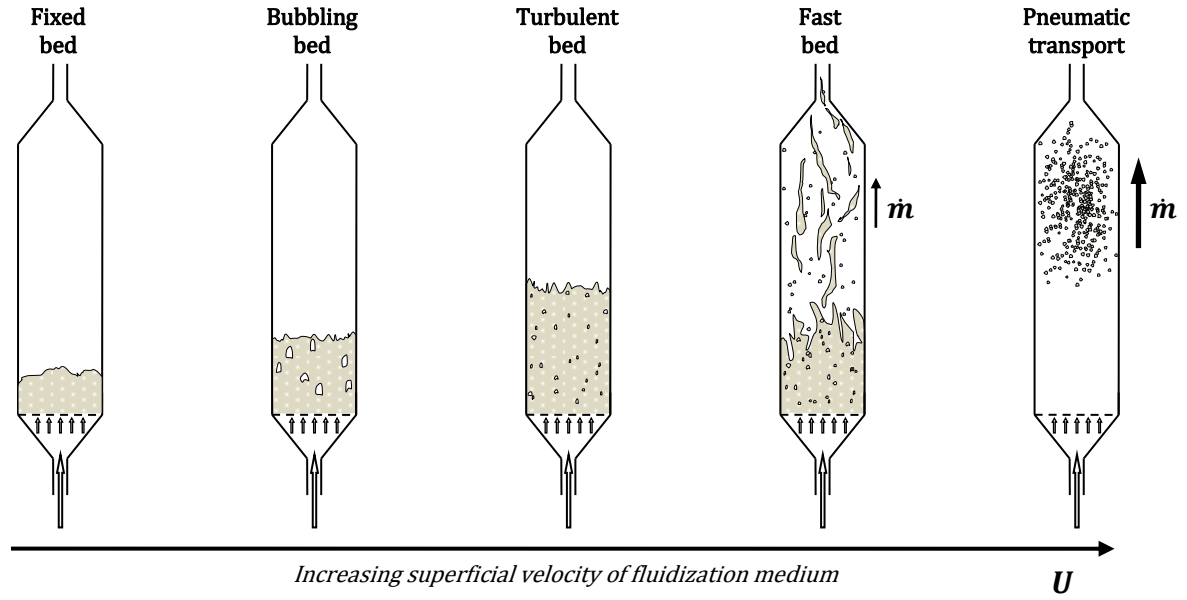

Figure 2-5. Fluidization states at varying velocity of fluidization medium.

2.2.3.1 Bubbling fluidized bed

When the gas velocity of the fluidization medium is lower than the minimum fluidization velocity, the bed does not lift. Such a state is prevalent in grate firing where primary combustion air is injected from under the bed. If the gas velocity is increased to the minimum fluidization velocity the particles present in the bed no longer adhere to each other. Here, the bed has reached the incipiently fluidized state (Basu, 2006). An increased gas velocity from this state results in the appearance of bubbles, marking the transition to the *bubbling fluidized bed* (BFB). A simplified schematic of a BFB for combustion is presented in Figure 2-6 (left).

If the gas velocity is increased to above that of the minimum fluidization velocity, the apparent volume of the bed increases as space between the particles increase. Turbulence becomes more pronounced and bubbles formed burst more frequently. Smaller particles and particles released upon bursting of bubbles are transported along the gas (Alvarez, 2006).

As long as the bed expands along with the gas velocity in a predictable manner, the bed is said to be in the bubbling state. As soon as a further increment of gas velocity results in an irregularity in bed expansion, the bed enters the turbulent fluidization state (Basu, 2006). The transition is due to bubbles progressively shrinking in size with increasing gas velocity until individual bubbles are hard to identify (Basu, 2006).

2.2.3.2 Fast fluidized bed

As gas velocity increase from the turbulent fluidization state, the bed position becomes increasingly less pronounced as particles leave the bed. At a high enough gas velocity, it is difficult to define the surface of the bed. The bed state where these conditions reign is referred to as the fast fluidized bed (Basu, 2006). Such conditions are typical to those in a *circulating fluidized bed* (CFB) reactor, where some bed material and partially oxidized fuel particles are transported along the gas stream to be continuously reintroduced to the bed after being separated from the flue gas in a cyclone (Alvarez, 2006). A CFB boiler is illustrated in Figure 2-6 (right).

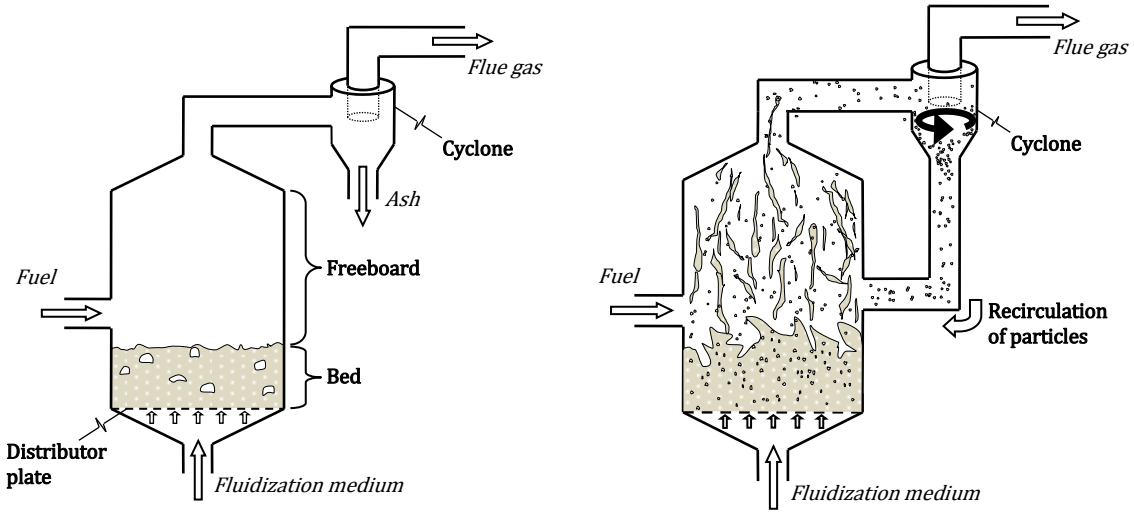

Figure 2-6. Simplified schematic of a bubbling fluidized bed boiler (left) and a circulating fluidized bed boiler (right) for fluidized bed combustion.

2.2.3.3 Pneumatic transport

If gas velocity is further increased from the fast fluidized state, the phase of pneumatic transport is reached when gas velocities reach the terminal velocity U_t (Basu, 2006). Here, all bed particles are entrained and transported along the gas stream while the mixing of solids is reduced (Basu, 2006). Like other transitions between bed fluidization states, the gas velocity where this phase change occurs is dependent on the size and weight distribution of the bed particles. The phase change to pneumatic transport is less pronounced than the one to e.g. bubbling fluidization. The fluidization state of pneumatic transport is used in boilers for combustion of pulverized coal but less frequently for unprocessed biomass (Basu, 2006).

2.2.4 Bed materials

For use in a FB reactor, in principle any inert material with an adequate and homogeneous particle size and weight distribution may be used as bed material. Since the material is prone to both chemical and mechanical wear, a low-cost material is of interest as the material will need to be continuously replaced. Besides a low cost and high availability of the material, there are a number of desired characteristics that define a good bed material:

- *High heat transfer capacity*

Since the primary purpose of a bed material is to carry heat between fuel particles, a high transfer capacity is desired. A high heat transfer capacity ensures sufficiently high heating rates and homogeneous temperature distribution and therefore good control of flue gas or product gas composition.

- *High melting point*

Even if fluidized bed reactors often are designed to operate in relatively low temperature ranges, it is required of a bed material to have a melting point above 1 000 °C, well above the temperature range of normal operation. This is to ensure no partial melting or softening of bed material occurs, which might otherwise be a cause of agglomeration.

- *Mechanically resistant*

Inherent in the fluidization process, the bed material is in constant motion. Due to the frequent collisions with particles and surfaces in the bed, abrasion of the bed particles is an issue. For this reason, the bed material should be mechanically resistant enough to withstand an acceptable length of time in the reactor.

- *No cause of erosion*

Although it is desired that the bed material is mechanically durable, the bed material itself should preferably not be a cause of erosion of reactor walls and in-bed heat exchanger surfaces.

- *Inert to ash-forming elements*

Chemical reaction or interaction with the bed material can give rise to operational problems. It is therefore of importance that the bed material is not prone to react with ash-forming elements.

The most commonly used bed material in fluidized bed reactors is silica sand. Its main constituent is SiO_2 (Lin et al., 2003). Although the material is of low cost and is abundant, it has been shown to react with K from biomass ash to form low melting point eutectics that subsequently lead to agglomeration. In order to minimize these problems, other bed materials are increasingly being used. Some of these bed materials are olivine (main composition of $(Mg,Fe)_2SiO_4$) and bauxite (main composition Al_2O_3) (Wolf et al., 2004, Mastellone and Arena, 2008). These bed materials have similar properties in that they are all mechanically resistant, have melting points higher than the normal temperatures applied in fluidized bed reactors and have high heat transfer capacities. The difference lies mainly in to what degree the bed materials react with ash-forming elements in the biomass fuel. For more details, refer to Section 2.4.1.

2.3 Thermal conversion of biomass in FB reactors

In this section, a summary of the most relevant concepts for thermal conversion of biomass fuel in fluidized beds are presented.

2.3.1 Gasification

The primary aim for gasification of biomass in a fluidized bed is the production of energy-rich gas. This gas can be directly combusted in a gas turbine to generate electricity and heat. Furthermore, the gas can be upgraded to transportation fuels such as biomethane or used in the production of high-value chemicals.

When a biomass particle is introduced into a hot FB reactor, it is dried when its temperature is ≥ 100 °C. Thereafter, the fuel particle undergoes devolatilization or pyrolysis when its temperature is > 300 °C. In this rapid process (typically completed in less than 1 minute), most of the fuel is converted. The main products at this stage are permanent gases, char and tar (Basu, 2006).

After devolatilization, the char is gasified with an oxidizing agent, e.g. steam and air. The main reactions that take place during gasification are:

- *Boudouard reaction:*
  $C + CO_2 \leftrightarrows 2\,CO$ +172.47 kJ/mol

Reaction 1

- *Water gas reaction:*
  $C + H_2O \leftrightarrows CO + H_2$ +131.3 kJ/mol

Reaction 2

- *Hydrogenating gasification reaction:*
  $C + 2H_2 \leftrightarrows CH_4$ -74.9 kJ/mol

Reaction 3

These reactions as well as the drying and devolatilization of biomass are endothermic or weakly exothermic. The other reactions that occur during biomass gasification are presented below:

- *Water-gas shift reaction:*
  $CO + H_2O \leftrightarrows CO_2 + H_2$ -41.2 kJ/mol

Reaction 4

- *Methanation of hydrogen and carbon monoxide:*
  $CO + 3H_2 \leftrightarrows CH_4 + H_2O$ -206.17 kJ/mol

Reaction 5

For the reactions presented in the present and subsequent sections, enthalpies of reaction were calculated based on enthalpies of formation extracted from the JANAF Thermochemical Tables, Third Edition (M.W. Chase Jr, 1985).

The concept of *cold gas efficiency* (μ_{cg}) is one of the main parameters that is used to assess the performance of a gasifier. Based on the energy content of the product gas compared to the fuel energy input, it is defined as (Basu, 2006):

$$\mu_{cg} = \frac{Q_{gas} \cdot \dot{m}_{gas}}{Q_{fuel} \cdot \dot{m}_{fuel}}. \tag{2.10}$$

Here Q_{gas} and Q_{fuel} denotes the *lower heating value* (LHV) of the gas and gasified fuel, while $\dot{m}_{gas}$ and $\dot{m}_{fuel}$ denotes the corresponding mass flows of gas and fuel crossing the system boundary of the gasifier.

2.3.1.1 Gasification medium

In FBG, the fluidization medium reacts chemically with the fuel according to the reactions stated in the previous section. For this reason, the fluidization medium in FBG is synonymous with gasification medium. Gasification of fuels can take place with air, oxygen, steam or carbon dioxide or a combination of these. When air is used during gasification the product gas is diluted with the nitrogen present in the air to around 50 % of total product gas volume (Basu, 2006). Gasification with oxygen or steam is therefore common, as product gas using these gasification mediums is free of nitrogen dilution and therefore of higher calorific value. Gasification in air typically yields a product gas of energy content 4–6 MJ/Nm^3, while gasification in steam or oxygen results in a gas of 10–15 MJ/m^3 (Basu, 2010).

The yield and composition of the product gas is affected among other factors by the ratio of the fuel to the gasification medium. In the case of steam gasification, this parameter is expressed as the ratio of the weight of steam introduced in the reactor to the weight of the biomass (Basu, 2010). By altering the *steam-to-biomass ratio*, the gas composition can be controlled (Lv et al., 2004). At a certain steam-to-biomass ratio the gasification system exhibits a peak in carbon conversion efficiency and gas production (Lv et al., 2004). A higher steam-to-biomass ratio results in a slightly higher gas yield and

a slightly lower tar content (Rapagna et al., 2000). The composition of the product gas is also influenced. With increasing steam-to-biomass ratio less CO is formed while CO_2 concentrations increase. Similarly, H_2 concentration increases slightly while CH_4 concentration is unaffected (Rapagna et al., 2000). Although gasification can be undertaken with steam-to-biomass ratios in a wide range between 0.5 and 2.5, a narrower range is more often used in practice (Basu, 2010). Two studies related to industrial fluidized beds applied steam-to-biomass ratios between 0.84–1.45 and 0.84–1.06, respectively (Larsson et al., 2013, Xu et al., 2006). Steam-to-biomass ratios within these bounds are common in industrial applications.

2.3.2 Combustion

The main product of gasification of combustion is heat, which can be used to generate electricity in a steam turbine. The heat can also be used as process heat or for district heating.

The combustion of biomass particles in a FB reactor follows the same sequence of events as for gasification, presented in the preceding section. The main differences are:

1. The volatile matter that is released during devolatilization is ignited and combusted.
2. The char resulting from devolatilization of the biomass is combusted instead of gasified, and char combustion is notably faster than char gasification.
3. Only air or oxygen is used as fluidization medium and is supplied in equivalence or excess compared to the stoichiometric demand for complete combustion of the fuel (Basu, 2006).

The following reactions typically occur during combustion:

- *Partial combustion with oxygen:*
  $C + ½O_2 \leftrightarrows CO$ -110.5 kJ/mol
  Reaction 6
- *Combustion with oxygen:*
  $C + O_2 \leftrightarrows CO_2$ -393.5 kJ/mol
  Reaction 7
- *Combustion of carbon monoxide:*
  $CO + ½\ O_2 \leftrightarrows CO_2$ -283.0 kJ/mol
  Reaction 8

2.3.3 Dual fluidized bed gasification

Biomass devolatilization and gasification of the generated char are both endothermic processes and thus a heat source is required to sustain the gasification process. If no external source of heat is applied to the gasification process, a fraction of the char will have to be combusted (Basu, 2006). When the combustion is carried out in the same reactor as gasification, the process is called *direct gasification*. In this case the product gas is diluted with nitrogen which lowers its heating value as mentioned in the preceding sections. This problem can be avoided by using oxygen as gasification medium. However, this requires an oxygen separation system and the associated cost may be undesirable.

A technology that is increasingly being applied to provide the heat for gasification without diluting the product gas is based on combustion of the char in a separate FB reactor. This is commonly called *dual fluidized bed gasification* (DFBG) (Corella et al., 2007). A plant based on this technology has been in commercial operation for more than 10 years in Güssing, Austria. The DFBG pilot plant GoBiGas in Gothenburg, Sweden is projected to produce 100 MW of biomethane from pelletized biomass by 2016.

DFBG is typically carried out in two interconnected fluidized bed reactors, where one is dedicated to gasification of fuel and the other to combustion of char. In the gasification reactor which is fluidized with steam, endothermic reactions occur. Here, the fuel is devolatilized after which the generated char is partially gasified. The unconverted char is transported, along with bed material, to the combustion

reactor. The transport is carried out in a manner which prevents gas transfer between the reactor vessels, e.g. through loop seals. In this second fluidized bed reactor the char is oxidized with air, releasing heat that raises the temperature of the bed material. The hot bed material is then transported back to the gasification reactor, providing heat necessary for the endothermic reactions. In this manner, the product gas is kept free of nitrogen while heat released from char combustion can supply the energy needed for the endothermic steam gasification of the fuel (Corella et al., 2007, Tchoffor et al., 2013). Gasification can be undertaken in the wide temperature range of 750–870 °C although temperatures between 810–850 °C are common during gasification for industrial DFBG (Kirnbauer et al., 2013, Pfeifer et al., 2011, Larsson et al., 2013). A simplified schematic of a DFBG reactor is presented in Figure 2-7.

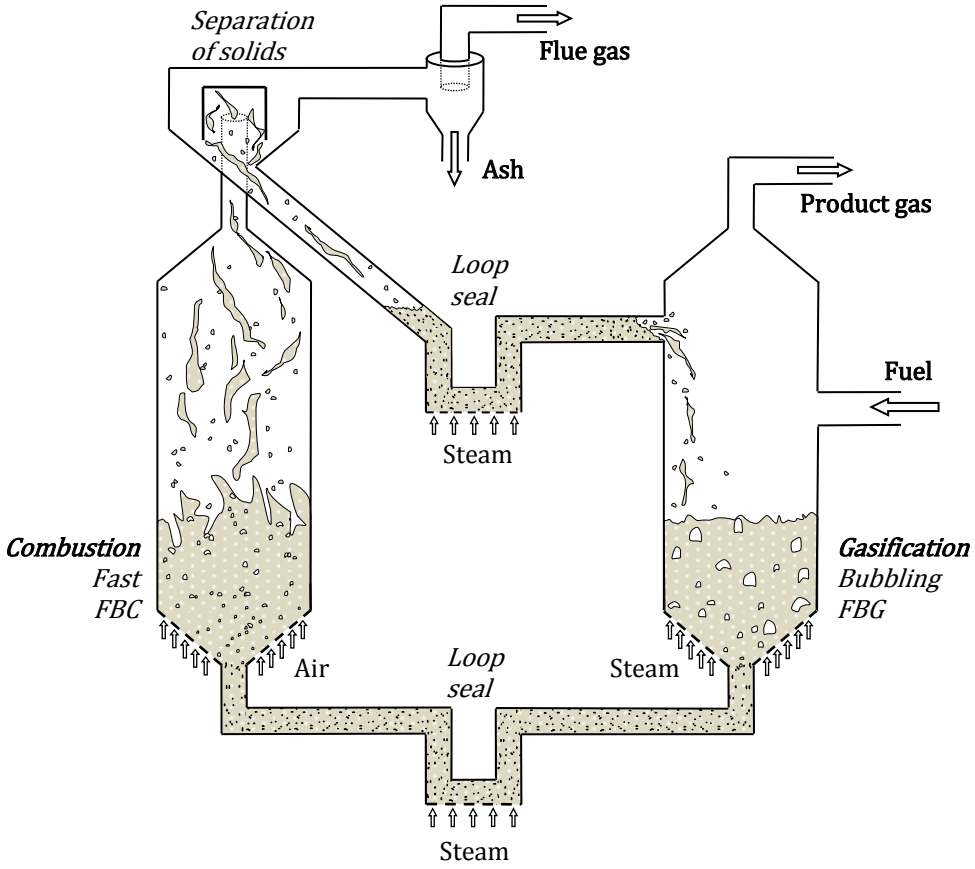

Figure 2-7. Simplified schematic of a dual fluidized bed gasification reactor.

2.3.4 Advantages of fluidized beds

Gasification and combustion in fluidized beds has proven to have notable advantages over more conventional methods of gasification and combustion of biomass fuels. Besides a nearly completely uniform temperature distribution in the fuel bed advantages include high fuel flexibility, short start up times, good scalability and low temperatures (Basu, 2006).

2.3.4.1 Uniform temperature distribution

Particle collisions are frequent in the fluidized state since the bed is in constant motion. The uniform temperature distribution renders less need for additional heating of the bed in order to ensure that a minimum temperature is reached in all bed regions, thus making a low process temperature possible. The constant circulation of bed material also results in excellent heat transfer between bed and heat exchanger surfaces (Alvarez, 2006).

2.3.4.2 Low temperatures

The low temperatures in FBG and FBC reactors can be achieved due to the heavy stirring inherent in the fluidization process, as the bed is in constant motion through stimulation from the fluidization gas stream (Roy and Sarma, 1970). Due to a lower combustion temperature normally ranging around 800–

900 °C, a FBC reactor exhibits low emissions of nitrous oxides (Alvarez, 2006). For FBG, reactor temperatures are slightly lower. The low temperatures reduce ash-related problems both in FBG and FBC since many ash-forming elements of low melting point can be kept in a solid state. Therefore, ash removal is simplified compared to other types of gasifiers or combustors (Basu, 2006). Fuels of high ash content or with content of low melting point ash-forming elements, such as biomass, is therefore suitable for thermal conversion in FB reactors.

2.3.4.3 Fuel flexibility

One prime feature of using fluidized beds in energy applications is its relative fuel flexibility, as the low fuel concentration in the bed material allows for varying water and ash content (Alvarez, 2006). Biomass is a highly heterogeneous fuel and fuel properties can vary between shipments, as can the availability of biomass over seasons. The possibility to gasify or combust different types of fuel or fuel mixtures therefore makes the usage of fluidized beds a good option for thermal conversion of biomass (Basu, 2006).

2.4 Ash transformation and release

During thermal conversion of biomass, volatile ash-forming elements in the fuel are released to the gas phase while less volatile or non-volatile ash-forming elements to a large extent remain in the char or ash. These elements undergo various transformations both in the gaseous and condensed phases. The compounds formed through transformation of ash-forming elements mainly result in undesired effects and give rise to ash-related problems in the reactor as well as in downstream processes (Tchoffor et al., 2013). Common negative effects include sintering, agglomeration of bed material, corrosion and fouling of heat transfer surfaces. However, some of the transformations of ash-forming elements contribute positively to the thermal conversion process. In this work, these effects are referred to as *ash-related benefits*.

2.4.1 Ash-related problems during thermal conversion processes

While the intention is that the bed material stays fully inert and unaffected of the thermal processes in the FB reactor, the ash-forming elements in the fuel may interact with the bed material and cause operational problems in the reactor and downstream equipment. Consequences may include reduced availability, damage of equipment and associated costs. Some of these problems are presented in the following sections.

2.4.1.1 Agglomeration

One of the most troublesome consequences of interaction between ash-forming elements and bed material is agglomeration. In this process, bed material particles adhere to each other to form an *agglomerate*, which may prevent mixing in the bed or lead to defluidization (Skrifvars et al., 1994, Lin et al., 2003)

Agglomeration may occur through the following mechanisms (Visser, 2004):

1) *Melt-induced agglomeration.* Molten ash-forming elements in liquid phase adhere to bed particle surfaces, acting like glue to form necks between bed particles. Composition of the molten phase is similar to the ash composition of the fuel.
2) *Coating-induced agglomeration.* The elements in the ash which have a low melting point are released to the gas phase. These elements coat bed material particles to form a uniform layer. If thick enough, the layer may form necks between bed particles.

The fuel ash content of K and Na is a key factor in the process of agglomeration (Dayton and Milne, 1995). Together with Si present in the bed material or ash, these elements form low melting point eutectic compounds of alkali silicates, e.g. potassium silicate, $K_2O \cdot 2SiO_2$. (Lin et al., 2003). For example, wheat straw ash has been shown to melt at 750 °C, a temperature well below the normal range of FBG operation (Lin et al., 2003).

Although Si based bed materials are more prone to cause agglomeration problems than other bed materials, ash melting problems might occur in fluidized bed reactors even if a non-silica based bed material is used. Compounds of low melting points can be formed from ash components alone if the fuel ash contains both K and Si in sufficient concentrations (De Geyter et al., 2007).

The *defluidization time* and *defluidization temperature* are commonly applied benchmarks to assess the tendency of various bed material and fuel combinations to result in agglomeration. The defluidization time describes the time of defluidization in relation to when fuel feeding was initiated. The defluidization temperature describes the upper temperature limit within which the bed can remain fluidized. If the defluidization temperature is lower than the operating temperature in a FB reactor, the fuel is difficult to handle in a FB application.

The following measures can be applied to mitigate agglomeration problems during thermal conversion processes (Basu, 2006):

- *Reducing the concentration of certain ash elements*

As has been previously mentioned, reducing the concentrations of K and Si can lower the risk of agglomeration as these elements may form low melting point eutectics. High concentrations of K in a fluidized bed reactor can be reduced or avoided by leaching the biomass fuel prior to thermal conversion or using a fuel with a low concentration of K such as wood pellets. High concentrations of Si in a fluidized bed can be reduced by using a fuel with a low concentration of Si such as wood pellets and/or a bed material with no or a very low concentration of Si.

- *Reducing the operation temperature*

If the operation temperature is kept below the melting points of ash, the risk of agglomeration occurring can be significantly reduced.

- *Promoting the formation of compounds of higher melting point*

Since agglomeration is the result of the formation of low-melting eutectic compounds such as potassium silicate, agglomeration problems can be reduced if the formation of compounds of low melting point is suppressed in favor of compounds with higher melting points. The presence of Al in the bed (as additive or a component in bed material) promotes the formation of alkali aluminosilicates (e.g. $K_2O{\cdot}Al_2O_3{\cdot}2SiO_2$) which have melting points above the normal range of FB operation (Aho and Silvennoinen, 2004). Compared to silica based bed material, the usage of Al-rich bed material such as bauxite has been shown to extend the defluidization time by 7 to 10 times (Vuthaluru et al., 1999). The presence of Fe has also been suggested to have similar effects through formation of $K_2Fe_2O_4$ with melting point above 1 135 °C (Werther et al., 2000).

Similar effects have been observed when P, Mg and Ca is present in the system. For example, the formation of phosphates of high melting point is possible if the P/K ratio is below 1.5–2 (Grimm et al., 2012). Molar ratios of relevant elements, *index ratios*, are frequently used in order to indicate whether a fuel mixture or a bed state is prone to agglomeration. The lower the molar ratio of (K+Na)/(Ca +Mg) in a biomass ash, the lower the risk of agglomeration (Sommersacher et al., 2011). Similarly, the lower molar ratio of Si/(Ca+Mg) in P poor systems and (Si+P+K)/(Ca+Mg) in P rich systems, the lower the risk of agglomeration (Grimm et al., 2012).

2.4.1.2 Fouling and slagging

Apart from agglomeration, fuels high in alkali or with ash of low melting point may disturb the operation of the FB reactor through fouling and slagging. During thermal conversion processes, volatile ash-forming elements such as K, Cl and S can be released from the fuel. Non-volatile elements such as Ca and Si can be entrained by the fluidization gas. If the released and entrained ash is deposited inside the reactor, slagging is said to occur. If the ash condenses on cooler surfaces downstream of the reactor, fouling is said to occur (Dayton and Milne, 1995, Miles et al., 1996). The

deposition reduces heat transfer capacity of heat exchangers and other surfaces, increasing the metal temperature which may shorten the reactor lifespan and increase maintenance needs (Basu, 2006).

2.4.1.3 Corrosion

Certain compositions of slag or fouling deposits are corrosive which may lead to wear on surfaces where fouling or slagging occurs (Basu, 2006). In addition, Cl-rich fuels pose a significant high-temperature corrosion potential (Basu, 2006). Alkali metals tend to react with chlorine to form alkali chlorides which are highly corrosive. Of this reason, methods that act to bind alkali in higher melting-point compounds are effective also to reduce corrosion problems. As previously presented, the presence of Al, Ca, Fe, Mg and P in the fuel or bed material can contribute to this effect.

2.4.2 Ash-related benefits during thermal conversion processes

A number of ash elements have been shown to exhibit desirable effects on thermal conversion processes. These effects occur when certain ash-forming elements are deposited on the bed material surface and act catalytically on certain reactions. A summary of the presented ash-related effects and the elements associated with these are presented in Table 2-3. For references, see Sections 2.4.1 and 2.4.2.

Table 2-3. Summary of ash-related effects and the responsible components.

Component in ash or bed material	Effect	Mechanism
CaO, Fe (and oxides)	Reduces tar content in product gas	Catalytic cracking of tars
Fe (and oxides)		Circulation of oxygen
CaO, Fe (and oxides)	Increases CO_2 and H_2 yield, decreases CO	Water-gas shift catalysis
Ca	Reduces risk of agglomeration	Increases ash melting point to retain alkali in solid form
Al		
P, Ca, Mg		
Si, K	Increases risk of agglomeration	Forms low-melting compounds
Cl, K	Increases risk of corrosion	Formation of KCl

2.4.2.1 Tar reduction

A reduction in tar content in the product gas has been noted when olivine is used as bed material during biomass gasification. The presence of CaO on the bed particle surface is thought to give rise to the catalytic effect (Kirnbauer et al., 2012).

CaO on the particle surfaces has been shown to accumulate during gasification of biomass to reach more than 10 times its original mass concentration, composing over 10 % of the bed material mass (Kirnbauer et al., 2012). Compared to fresh olivine, a CaO-coated olivine bed material exhibited better tar decomposition properties as the tar content of the product gas was decreased by 82 % (Kirnbauer et al., 2012).

Metallic iron and its oxides FeO, Fe_2O_3 and Fe_2O_4 also exhibit catalytic tar cracking properties (Abu El-Rub et al., 2004). However, in a DFBG system the exhibited tar reduction could also be attributed to the iron oxides of the bed material circulating oxygen from the combustion stage to the gasification stage. In this manner a fraction of the tars formed during gasification might then be combusted along with some amount of the product gas, resulting in a tar reduction at the cost of a lower product gas yield.

2.4.2.2 Water-gas shift catalysis

The presence of CaO on bed particles has been observed to favor the water-gas shift reaction (Reaction 4) resulting in a higher hydrogen and carbon dioxide content and a lower carbon monoxide content in the product gas (Kirnbauer et al., 2012). Additionally, iron and iron oxides have been reported to catalyze the water-gas shift reaction (Abu El-Rub et al., 2004).

3 Materials and methods

3.1 Method

The method applied involved 3 steps. Step one consisted of a literature review on ash transformation chemistry and FB processes such as the DFBG process. In addition to identifying gaps in knowledge, the aim of this step was to select appropriate bed materials, biomass fuels and reactor operation conditions to be applied in the experimental investigations.

In step two, experiments were conducted using a laboratory-scale fluidized bed reactor. The reactor was operated under well controlled conditions that were defined with information obtained from step one. During the experiments, the fuels studied were gasified and the resulting char was subsequently combusted. The gas exiting the reactor was analyzed. The bed material was sampled either during the experiment or at the end of the experiment.

In the third step, the ash-forming elements from the fuels retained on the outer layer of the bed material coating was analyzed. Possible connection between the characteristics of this layer and positive/negative effects of ash transformation on the DFBG process was studied. In Figure 3-1 a schematic of steps 2 and 3 of the applied method is presented.

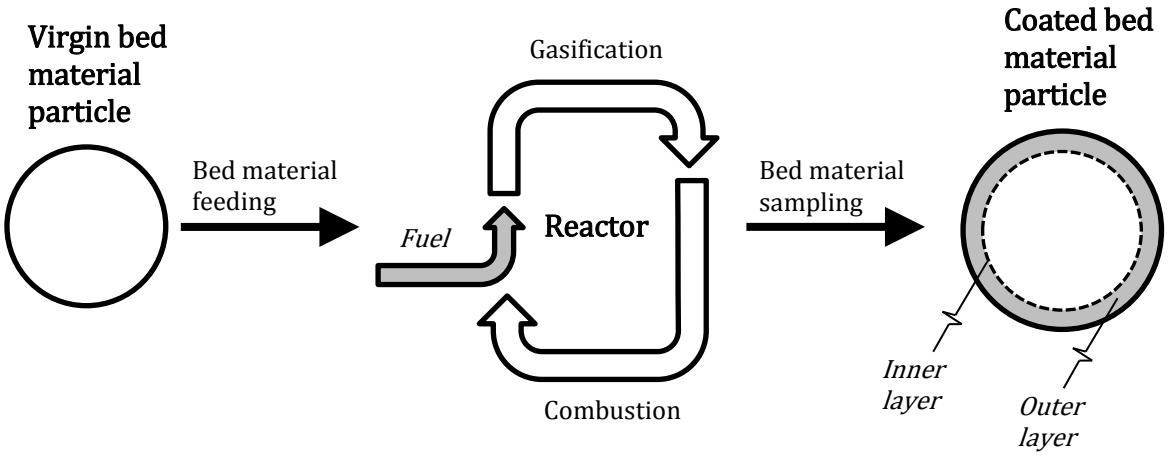

Figure 3-1. Illustration of bed material particle coating.

3.2 Fuels

Wheat straw (*Ws*) and forestry residues (*Fr*) were the biomass fuels studied. As previously mentioned, these fuels both present a somewhat untapped biofuel potential as these biomass fuels have traditionally been used for non-energy purposes or simply left after harvesting.

The forestry residue was sampled from the Sävenäs CHP plant in Gothenburg, Sweden. In order to ensure that the samples used during the experiments were homogeneous, the forestry residue was milled, well mixed and pelletized. The commercial wheat straw used was received in pelletized form and was free from additives and binding agents according to the manufacturer. In order to ensure homogeneity also of this fuel the wheat straw pellets were again milled, well mixed and pelletized. All pellets produced had a diameter of 8 mm. Necessary moisture for binding the pellets was added using distilled water. For further details regarding fuel preparation, see Appendix A.

The ash composition of the fuels is presented in Figure 3-2. In certain experiments, mixtures of forestry residue and wheat straw were applied through alternately feeding the reactor with pellets of Ws and Fr. The fuel mixtures were denoted *20%Ws* and *33%Ws*, respectively. The first mixture, 20 wt% wheat straw to 80 wt% forestry residue, yielded a total K concentration close to twice that of

pure forestry residues. The second mixture, 33 wt% wheat straw to 66 wt% forestry residues, yielded a total K concentration half of that of pure wheat straw.

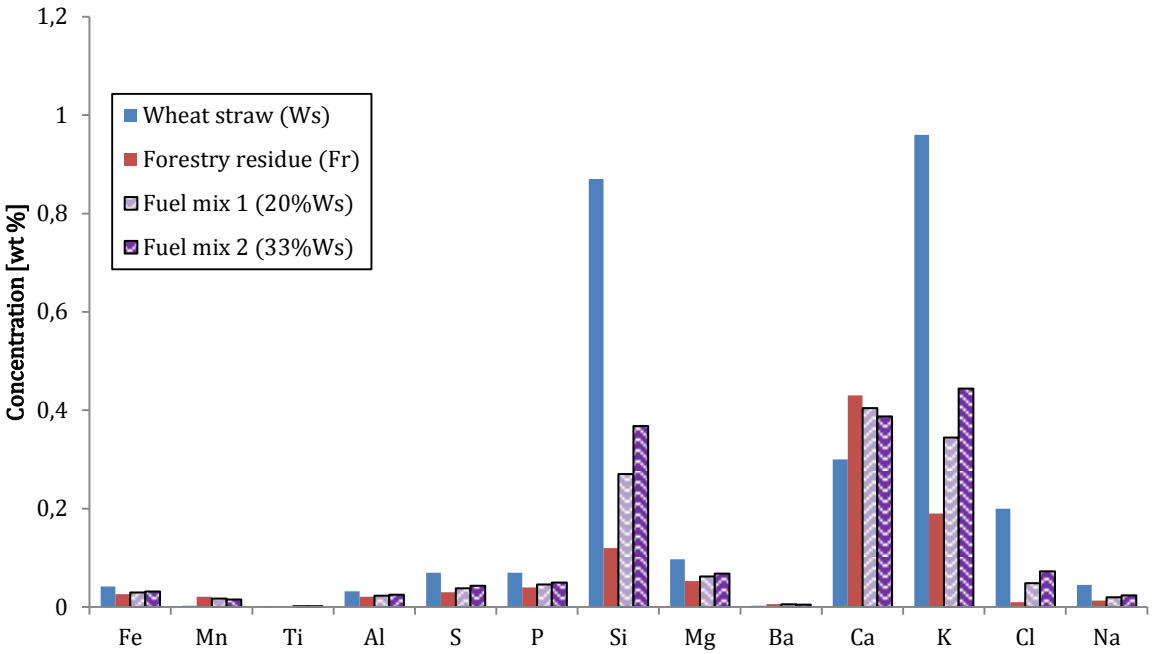

Figure 3-2. Ash composition of the fuels.

3.3 Bed materials

Three bed materials were selected: silica sand (Sa), olivine (Ol) and bauxite (Bx). As discussed in Section 2.2.4 and Section 2.4.1, silica sand is one of the most commonly used bed materials in fluidized bed reactors. However, due to a high Si content this bed material is prone to agglomeration problems when alkali-rich fuels are used, see Section 2.4.1.1. In this work, silica sand was chosen to act as a reference for agglomeration tendency. Both olivine and bauxite have far lower contents of Si than silica sand (see Figure 3-4) and are thus less likely to cause agglomeration problems. Therefore both olivine and bauxite are promising bed materials which can be used in a DFBG process and were thus selected to be studied. The bed materials used are presented in Figure 3-3.

Figure 3-3. The prepared bed materials and fuels used. Upper row: sand (left), olivine (center) and bauxite (right). Lower row: forestry residue pellets (left) and wheat straw (right).

The olivine and bauxite were provided by project partners while the sand used was commercial quartz sand of the trade name Baskarpsand 35. The sand particles as received had a SMD of 350 µm as stated by the manufacturer.

As received, the bed materials varied substantially in size. The three bed materials all had a size distribution that practically would have enabled their direct usage in the reactor since they all fulfilled the criteria for Geldart particles type B. However, in order to avoid any uncontrolled loss of finer particles through entrainment during the experiments, all bed materials were sieved to attain a target particle diameter of $250 \leq d < 500$ µm. The fractioning method and the sieve analysis of the fractioned materials are presented in Appendix B.

The chemical composition of bed materials determined through standard chemical analysis is presented in Figure 3-4. The full results of the lab analysis are presented in Appendix C, along with an account of the analysis methods used to obtain the analysis results.

Since the ash-forming elements from the biomass fuels are deposited on the surface of the bed materials during thermal conversion, the surface of the bed material particles were also analyzed. In Figure 3-5 the elemental composition of the bed material particle surfaces, as analyzed through XRF, is presented.

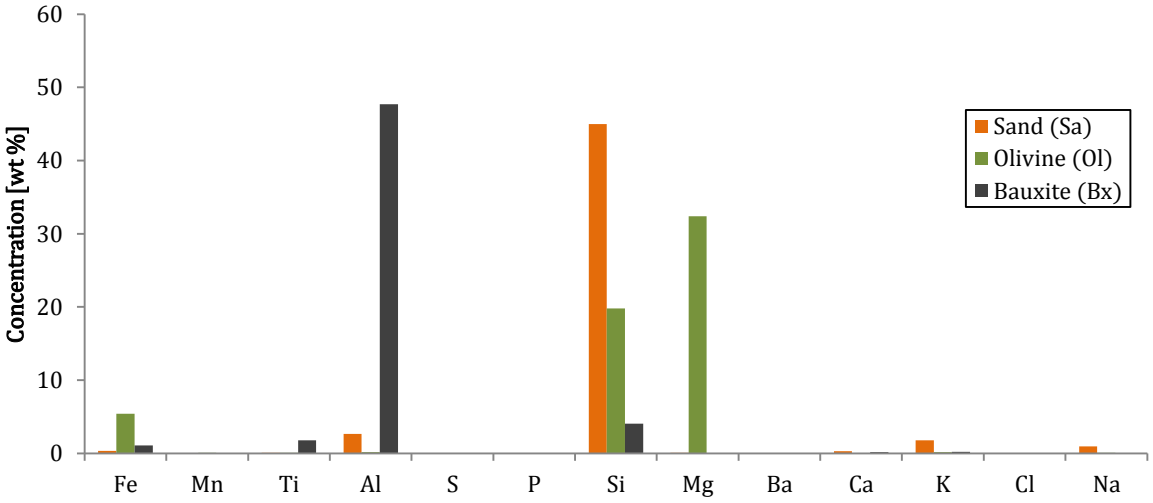

Figure 3-4. Elemental composition of bed materials measured with standard chemical analysis.

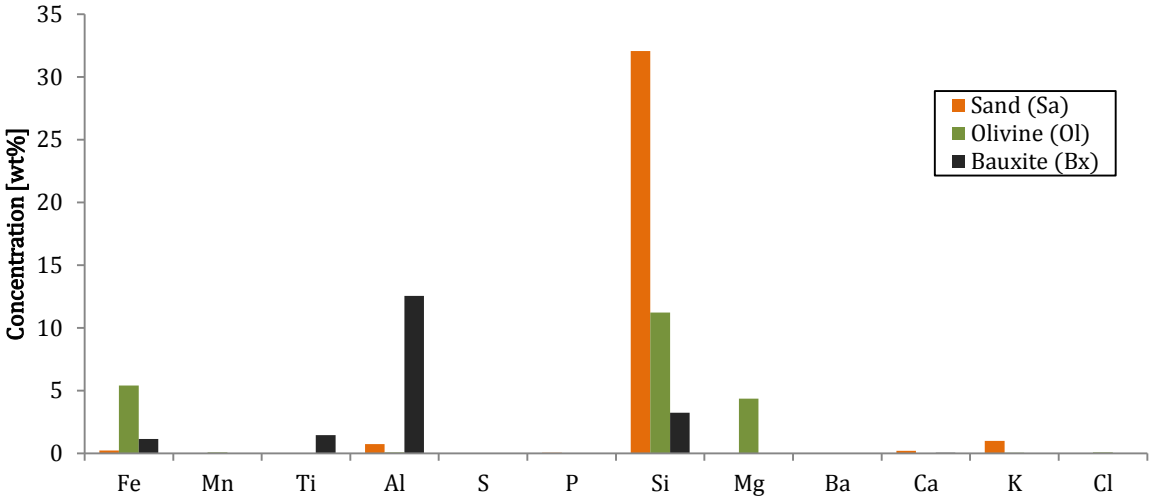

Figure 3-5. Elemental composition of bed material surfaces measured with XRF analysis.

3.4 Experimental setup

The experiments were carried out in a laboratory-scale BFB reactor. The cylindrical reactor which has a diameter of 7 cm and a length of 144 cm is divided into two sections by a perforated ceramic distributor plate (see Figure 3-6). The lower section, which is 62 cm in length, functions as a gas preheater. The bed material rests upon the distributor plate which is situated directly above the gas preheater. The upper section functions as the freeboard. Near the distributor plate is a bed material sampling system. Fuel was fed manually from the top of the reactor.

The reactor was electrically heated with surrounding heating elements which were controlled with a temperature regulator. The bed temperature was measured with a K-type thermocouple submerged in the bed. The pressure drop over the bed was monitored through a pressure sensor resting on the distributor plate. The pressure sensor was connected to a manometer.

The gas exiting the reactor was analyzed with *nondispersive infrared* (NDIR)/paramagnetic (for O_2) gas analyzers connected downstream the reactor. For details on principles of measurement, refer to Appendix D. The experimental setup is illustrated in Figure 3-6.

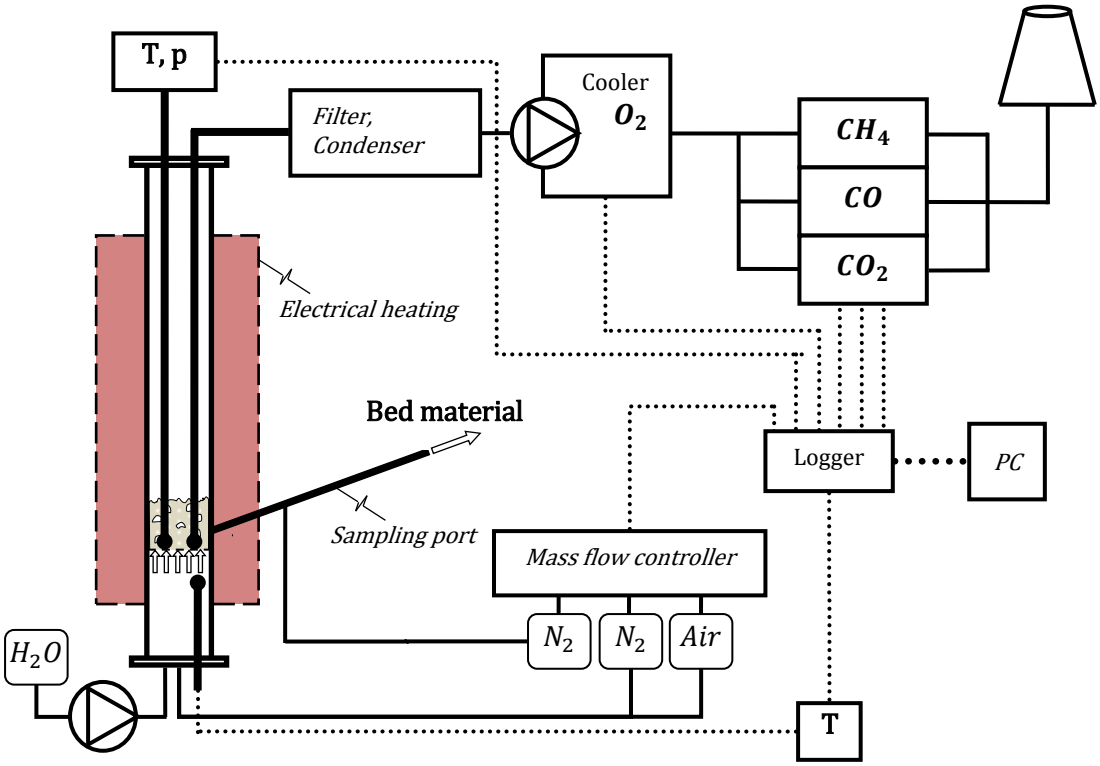

Figure 3-6. Schematic of the experimental setup. Solid lines indicate physical flows, dotted lines indicate flows of data.

3.5 Experimental design

Three sets of experiments were carried out:

Set i. Here the aim was to compare the propensity of the three bed materials to retain ash-forming elements from biomass fuels under conditions relevant to DFBG. To achieve this, experiments were carried out in which biomass was thermally converted under similar conditions with each of the three bed materials. At the end of each experiments the bed material was sampled and analyzed. The biomass fuels used in these experiments were 1) forestry residues and 2) a mixture of forestry residues and wheat straw (consisting of 20 wt% wheat straw and 80 wt% forestry residues).

Set ii. Here the effect of the atmospheres surrounding the fuel particles (during gasification and combustion) on the retention of ash-forming elements on the bed material was studied. An experiment was carried out with forestry residues and olivine under conditions relevant to DFBG. During the experiment the bed was sampled at the end of the gasification and char combustion stages. After the last sample was taken, the bed temperature was increased steadily in order to determine the agglomeration temperature of the residual ash.

Set iii. Here, the agglomeration tendencies of the three bed materials was investigated under conditions relevant to DFBG. Experiments were carried out in which biomass was thermally converted under similar conditions with each of the three bed materials. The time taken for agglomeration to occur in each experiment was determined. The main fuel used in this experiment was wheat straw. In order to study the effect of K concentration in biomass on agglomeration tendency, a mixture of wheat straw and forestry residue consisting of 33 wt% wheat straw (33%Ws) was also used. The concentration of K in this mixture was twice that of the pure forestry residue.

The experiments carried out are summarized in Table 3-1.

Table 3-1. Summary of the experiments performed.

Set	Aim	Fuel	Bed material	Denotation	Experiments performed	Temperatures [°C]	
						Gasification	Combustion
i	Investigate the tendency of bed materials to retain ash-forming elements	Forestry residue	Sand	Fr+Sa	1	860	890
		Forestry residue	Olivine	Fr+Ol	3	860	890
		Forestry residue	Bauxite	Fr+Bx	2	860	890
		20 wt% Straw/forestry res. mixture	Olivine	20%Ws+Ol	1	860	890
ii	Investigate the effect of gasification and combustion atmospheres on the accumulation of ash-forming elements on bed material	Forestry residue	Olivine	ii,Fr+Ol	1	860	890 (+ temp. ramping)
iii	Investigate agglomeration tendency of bed materials	Straw	Sand	Ws+Sa	1	860	890
		Straw	Olivine	Ws+Ol	1	860	890
		Straw	Bauxite	Ws+Bx	2	860	890
		33 wt% Straw/forestry res. mixture	Olivine	33%Ws+Ol	1	860	890

3.6 Experimental procedure

All experiments consisted of several cycles of gasification and combustion. Each cycle consisted of a gasification stage in which a given virgin biomass fuel was gasified followed by a combustion stage in which the unconverted char from the gasification stage was combusted.

The combustion and gasification stages of each cycle were carried out as follows:

a) Gasification stage. During the gasification stage of each cycle, the reactor was initially set to 860 °C. The reactor and bed material sampling system were purged with nitrogen to ensure an inert environment in the reactor. Distilled water was pumped in a controlled rate into the steam generator located in the gas preheater section of the reactor, producing steam. The preheated steam entered the bed of the reactor through the distributor plate. When the conditions in the reactor met the target values, biomass pellets were fed manually at a controlled rate into the reactor. During the fuel period which lasted 4 minutes, 277 g was fed into the reactor. The steam-to-biomass ratio was maintained at 0.9 during each experiment. For more details, see Appendix Table E-1. Due to the endothermic nature of gasification, the bed temperature dropped during this period. In most cases the temperature dropped to around 800 °C. See Appendix E for details.

b) Combustion stage. After the gasification stage of each cycle, the fluidization gas was switched from steam to air consisting of 6 vol% O_2. The low O_2 concentration was chosen in order to avoid a sharp increase in the bed temperature above the target combustion temperature of 890 °C. As a result of the low O_2 concentration, the unconverted char was combusted for a longer period of time (12 minutes) than the 4 minutes allowed during the gasification stage. This was to ensure that the unconverted char from the gasification of the biomass fuels was

completely or close to completely combusted. During char combustion the temperature rose above the target temperature of 890 °C . See Appendix E for details.

At the end of the char combustion stage of each cycle, the fluidization gas was switched from air to nitrogen to create an inert atmosphere in the reactor. The reactor was manually cooled down to 860 °C. When the conditions in the reactor again reached target parameters, steam was introduced in the reactor and a new gasification stage was carried out as described in a). At the end of this stage, a new combustion stage was carried out as described in b). The cycling is illustrated in Figure 3-7.

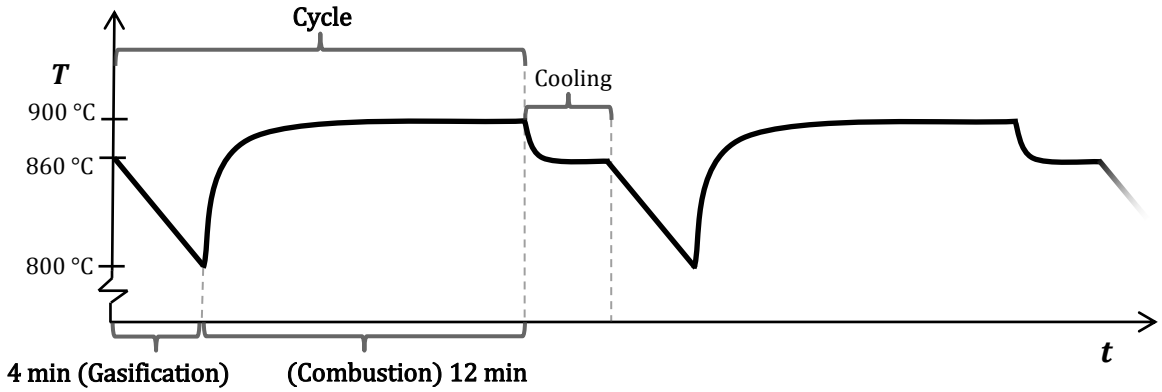

Figure 3-7. Illustration of the gasification and combustion periods forming cycles.

The number of cycles carried out varied across sets of experiments.

For the *set i* experiments (See Table 3-1), 6 cycles were carried out. The total experimental time was 2–2.5 hours. At the end of the 6th cycle, the fluidization gas was switched from air to nitrogen gas. The bed was sampled through the sampling port and the samples taken were cooled in a stream of nitrogen.

For the *set ii* experiment, 3 cycles were carried out. The total experimental time was 1 hour and 20 minutes. The bed material was sampled at the end of each gasification and combustion period. After the last sample was taken at the end of the 3rd cycle, the residual char was combusted and the bed temperature was increased in order to determine the agglomeration temperature.

For the *set iii* experiments, the number of cycles carried out was increased until the bed defluidized. The total experimental time was 0.5–2 hours. Samples of the agglomerated beds were taken after the reactor was let to cool in air.

For data on actual flows of fluidization gases and fuel in the experiments, see Appendix E. For details on the calculation of the operating parameters, see Appendix F. Example logger data for a *set i* experiment is presented in Appendix G.

3.7 Analysis of bed materials

The outer layer of the bed material particles sampled in the experiments were analyzed using XRF. Prior to analysis, char particles were separated from the bed material samples with sieves. A sieve of aperture size of approximately 1 mm separated large char particles and agglomerates from the bed material. A sieve of aperture size 500 µm was applied to separate fine char particles from the bed material. A few char particles < 500 µm could still be observed in the bed material samples after the sieving process.

4 Results

4.1 Propensity of bed materials to retain ash-forming elements

The results presented in this section are those of the set *i* experiments described in Section 3.5.

In Figure 4-1 the elemental composition of the outer layer of the bed material particles are presented for the virgin and the used olivine. The ash-forming elements from the forestry residues that were retained to the largest extent on the bed material particle surfaces during thermal conversion were Fe, P, Ca and K in the case of olivine. In the case of bauxite, the ash-forming elements that were retained to the largest extent were P, Mg, Ca and K, see Figure 4-2. In the case of sand, Ca and K were retained to the largest extent on the particle surfaces, see Figure 4-3.

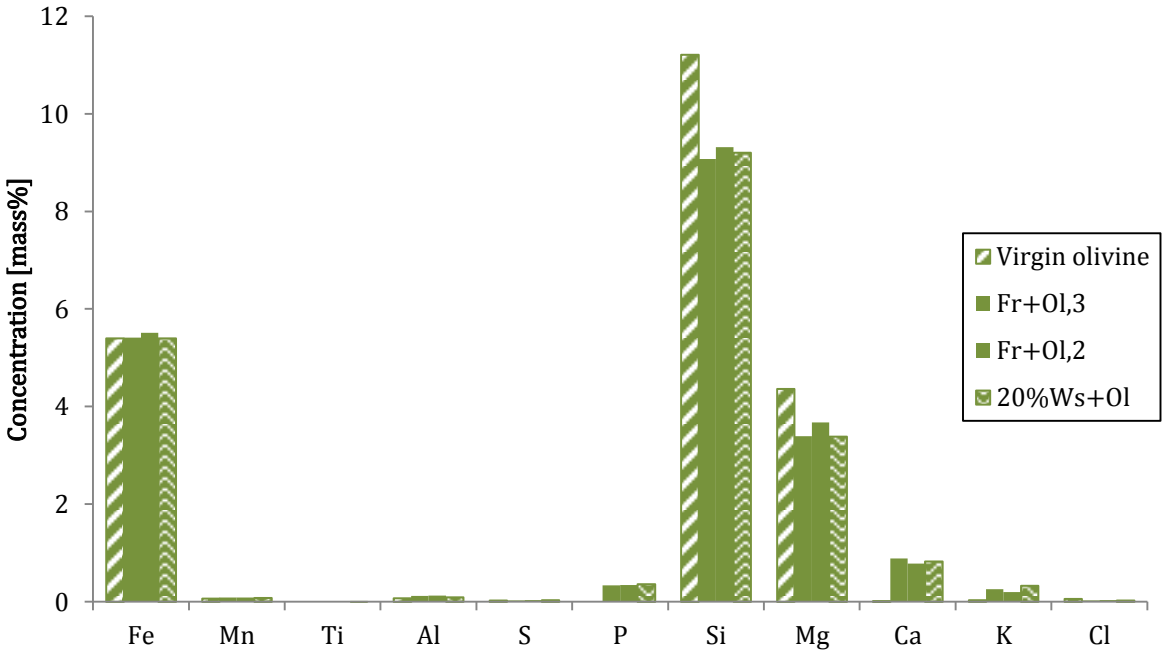

Figure 4-1. Elemental composition of the outer layer of the virgin and used olivine.

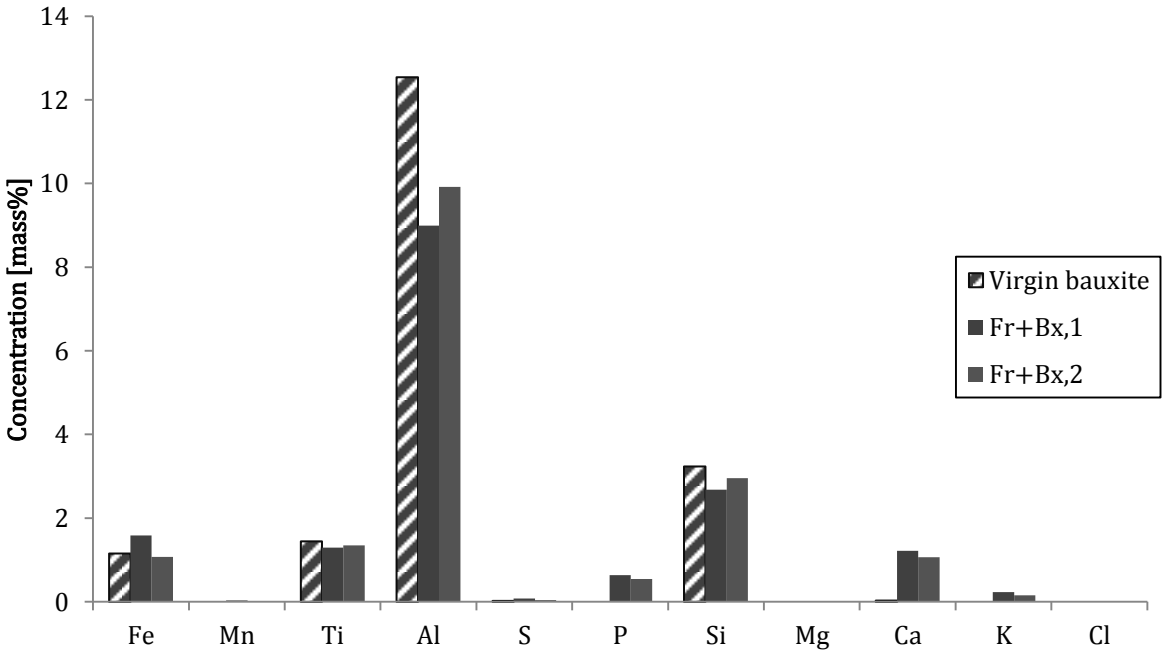

Figure 4-2. Elemental composition of the outer layer of the virgin and used bauxite.

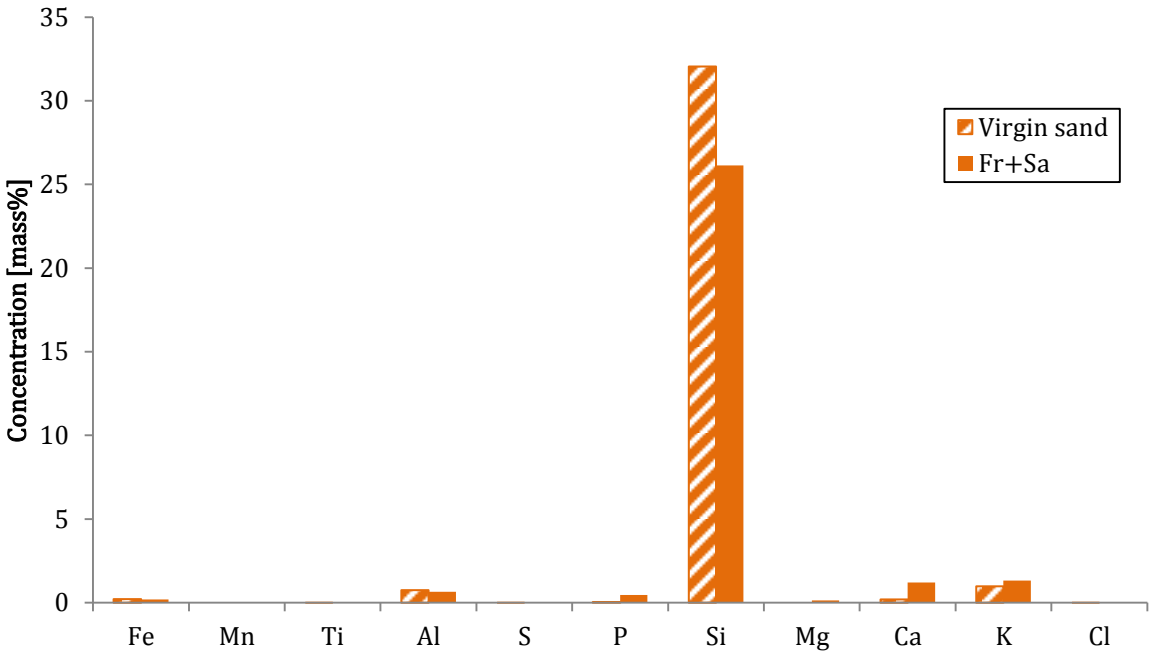

Figure 4-3. Elemental composition of the outer layer of the virgin and used sand.

The results presented in previous paragraph indicate that the main ash-forming elements from the forestry residue that were retained on the bed materials were Ca, K and P. In order to compare the intrinsic propensity of each of the three bed materials to retain the aforementioned ash-forming elements, the concentration of these elements on the surface of the virgin bed materials were subtracted from their corresponding concentrations on the used bed materials. The result obtained of this subtraction (see Figure 4-4) represents the amount of ash-forming elements from the forestry residues that were deposited on the surface of each of the bed materials. The result of this subtraction is presented for all elements in Appendix H.

It can be inferred from Figure 4-4 that bauxite and sand have a similar propensity to retain Ca on their surfaces during thermal conversion of biomass fuels. Both bed materials have a higher propensity to

retain Ca than olivine. P is retained to the highest extent on bauxite followed by sand and olivine. Sand retains K to the largest extent followed by bauxite and olivine.

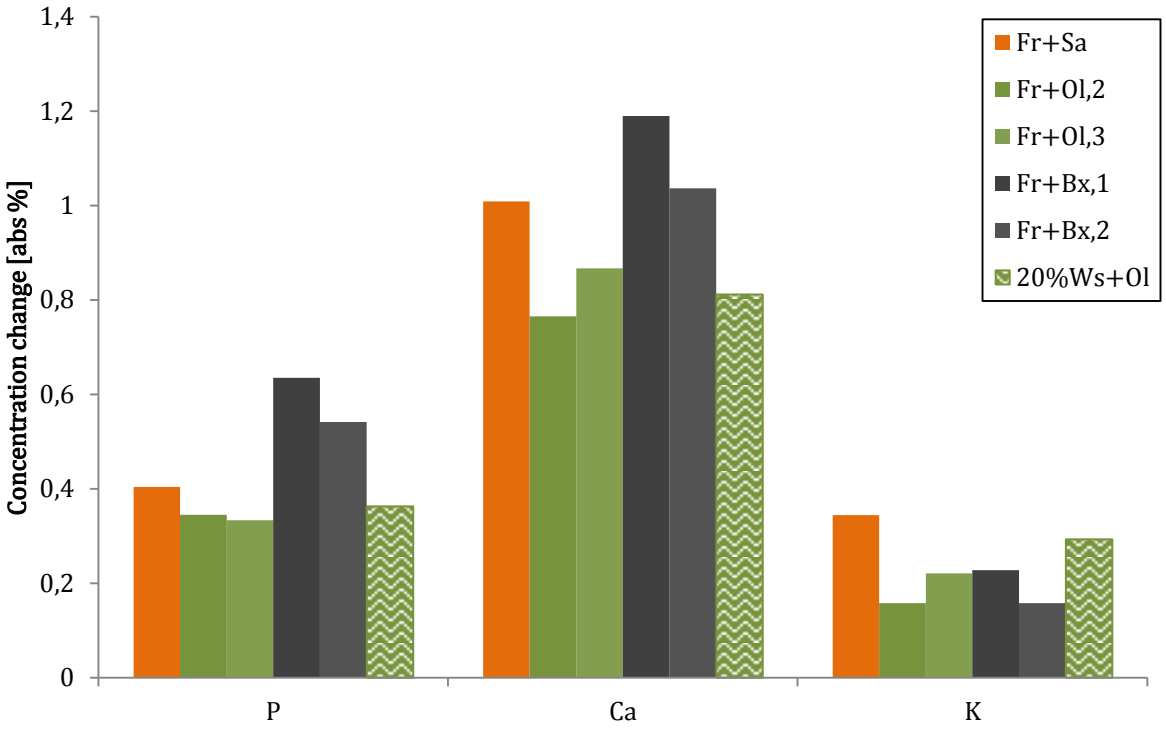

Figure 4-4. Change in surface concentration of ash-forming elements on the bed material particles during the set *i* experiments. The presented values are averages of 2 to 3 replicate analyses of each sample.

To verify that no significant amount of bed material particles were entrained from the bed during the experiments, a reference experiment using olivine was carried out under the same conditions as the set *i* experiments but with the exception that no fuel was fed to the reactor during the experiment. More than 99,5 % of the initial bed material weight was recovered at the end of the experiment. Thus, the entrainment of olivine particles did not significantly affect the concentration of ash-forming elements. It can be assumed that the other bed materials behaved in a similar manner since they were of similar size distribution: see Appendix B and Appendix F.4 for details.

4.2 Effect of atmosphere on ash-forming element retention

The results presented in this section were obtained from the set *ii* experiments described in Section 3.5. The effect of the surrounding atmosphere in the reactor on the retention of ash-forming elements from the forestry residues on the surface of olivine particles is shown in Figure 4-5. In this figure, G1 and C1 respectively denote the gasification and combustion stages of the first cycle during the experiment. Similarly, G2 and C2 denote the gasification and combustion stages of the second cycle during the experiment. G3 and C3 follow the same pattern. G0 denotes the sample taken before fuel feeding was started.

It can be seen in Figure 4-5 (center) that the concentration of Ca on the surface of the olivine particles increased after each char combustion stage (C1, C2 and C3) and remained virtually unchanged during each gasification stage (G1, G2 and G3). This indicates that Ca was mainly retained on the surface of the olivine particles during char combustion. Similarly, P was mainly retained on the surface of the olivine particles during char combustion, see Figure 4-5 (left). K was to some extent retained on the surface of the olivine particles during both gasification and combustion, see Figure 4-5 (right).

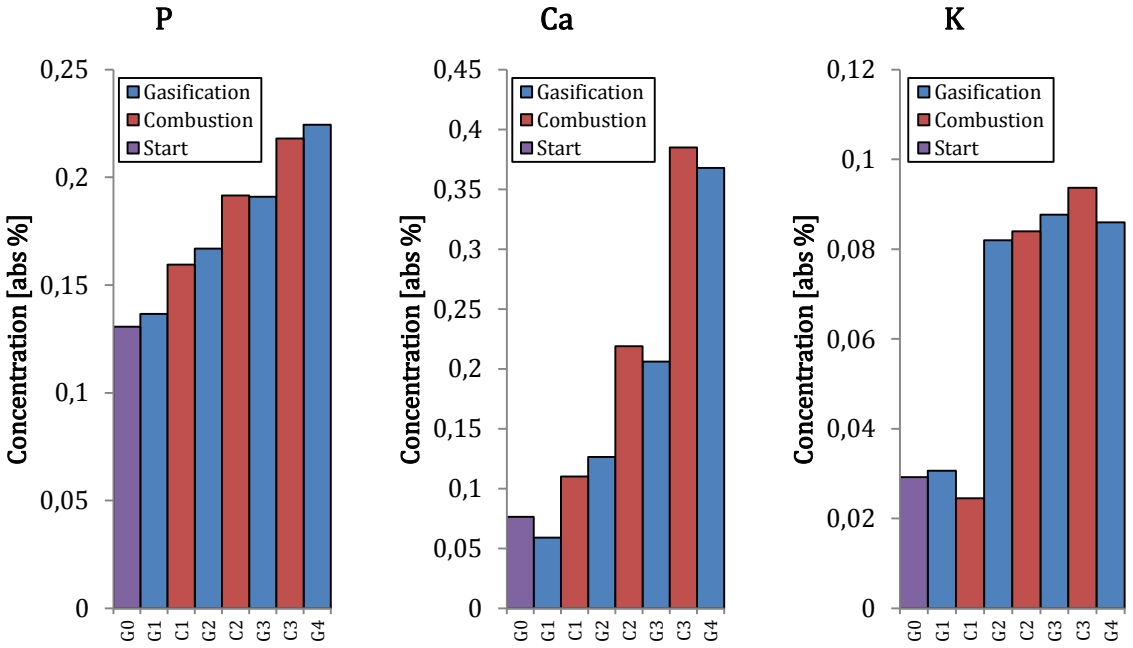

Figure 4-5. P, Ca and K concentrations on the outer layer of the olivine particles sampled during the ii,Fr+Ol experiment. The presented values are averages of 2 to 5 replicate analyses of each sample.

4.3 Agglomeration resistance

The results presented in this section were obtained from the set *iii* experiments described in Section 3.5.

The time taken for defluidization to occur during each experiment is presented in Table 4-1. This time represents the time at which the bed defluidized as compared to the start of the experiment, not including the time taken to switch from gasification to combustion and vice versa as this varied between experiments.

Table 4-1. Set *iii* experiment results.

Fuel-bed material combination	Defluidization on cycle no.	Defluidization time (minutes)
Ws+Sa	2	19.7
Ws+Ol	3	44.8
Ws+Bx,2	2	23.9
33%Ws+Ol	6	92.0

From the defluidization times shown in Table 4-1 it can be inferred that bauxite and sand have similar resistance to agglomeration and that both of these bed materials are less resistant to agglomeration than olivine.

An attempt was made to determine the agglomeration temperature of olivine (see set ii experiments described in Section 3.5. At a bed temperature of 1 025 °C, the bed did not agglomerate. The experiment was stopped at this temperature as it was close to the maximum temperature (1 100 °C) the reactor could handle.

4.4 Concentrations of CO, CO_2 and CH_4 in the product gas

The concentration of CO, CO_2 and CH_4 in the product gas resulting from the gasification of forestry residues (set *i* experiments described in Section 3.5) with each of the bed materials olivine, bauxite and sand are presented in Figure 4-6 to Figure 4-8. The presented data points where CH_4 concentration

exceeds 10 % are estimations, as the span of the methane instrument was limited to 10 %. However, the instrument displayed estimates of methane concentration even when above this range, and these values were noted manually. Refer to Appendix I for details.

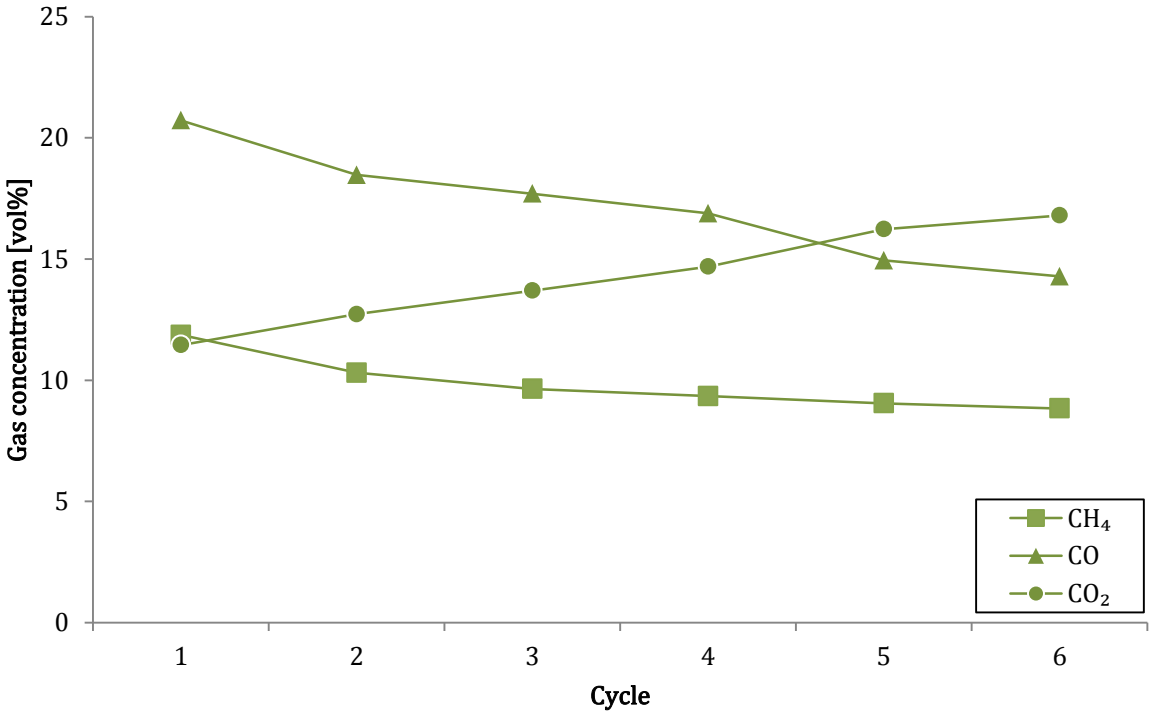

Figure 4-6. Product gas concentrations during gasification of forestry residues using olivine as bed material. The maximum standard deviations in the concentrations of CO_2, CO and CH_4 calculated in 3 replicate experiments were respectively 1.8, 0.9 and 0.6 vol%.

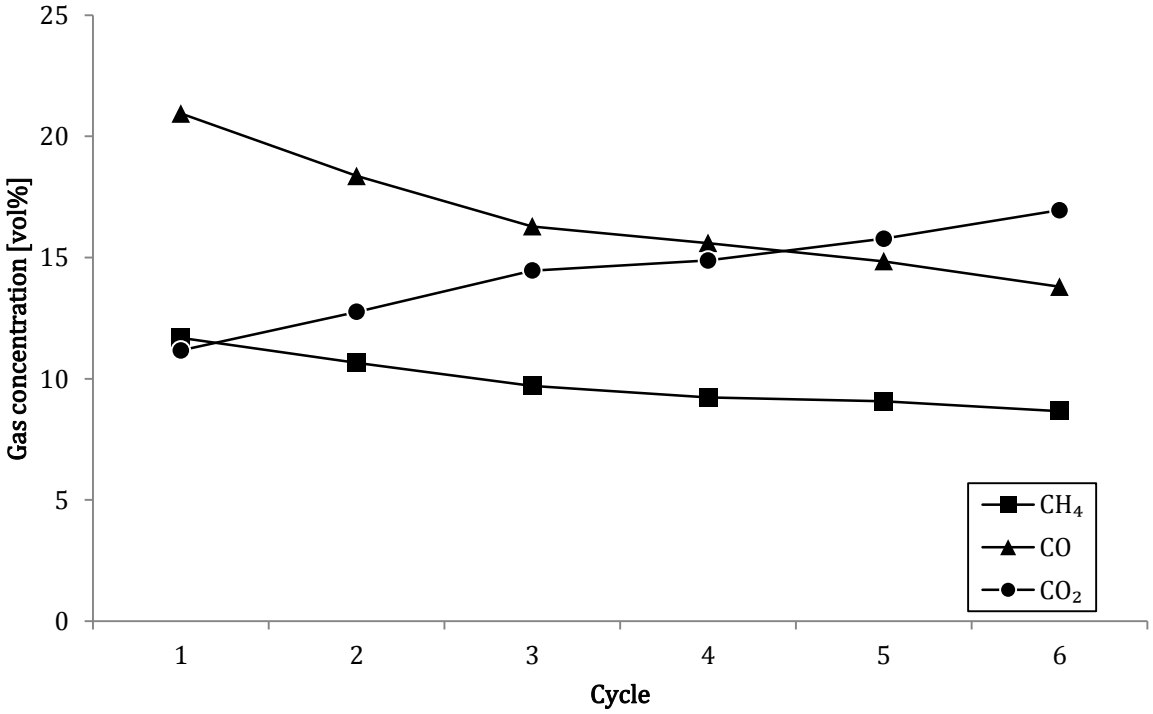

Figure 4-7. Product gas concentrations during gasification of forestry residues using bauxite as bed material. The maximum standard deviations in the concentrations of CO_2, CO and CH_4 in 2 replicate experiments were respectively 1.9, 2.9 and 0.4 vol%.

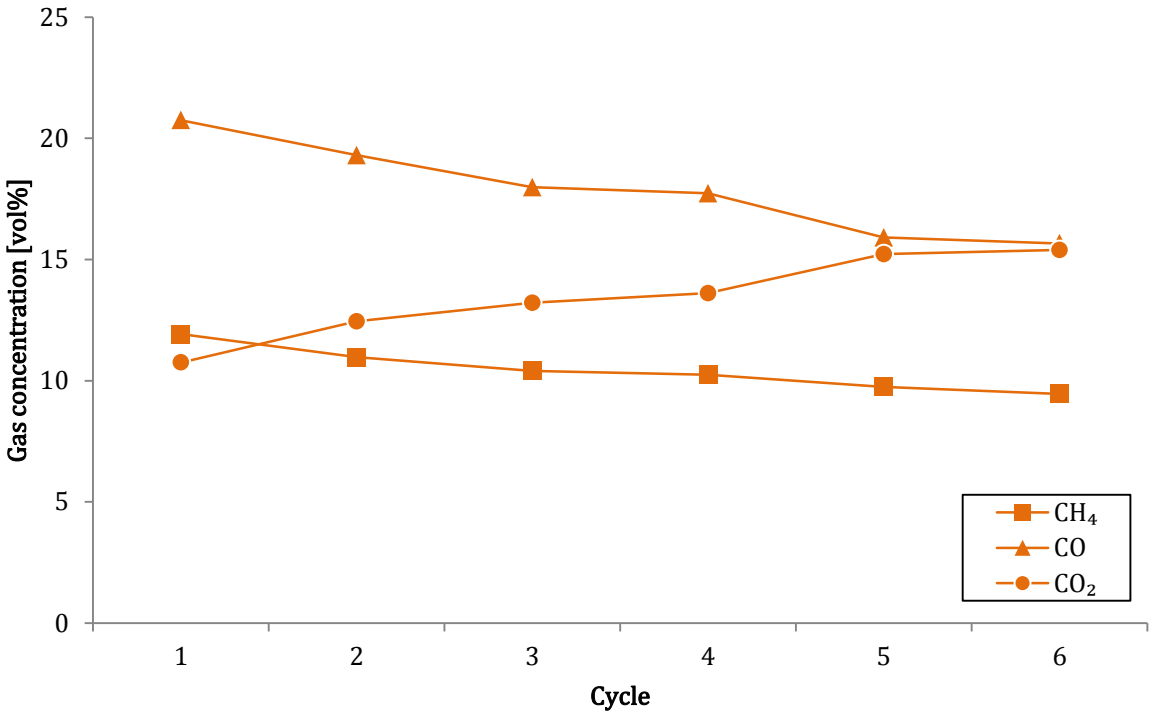

Figure 4-8. Product gas concentrations during gasification of forestry residues using sand as bed material. Only a single experiment was performed.

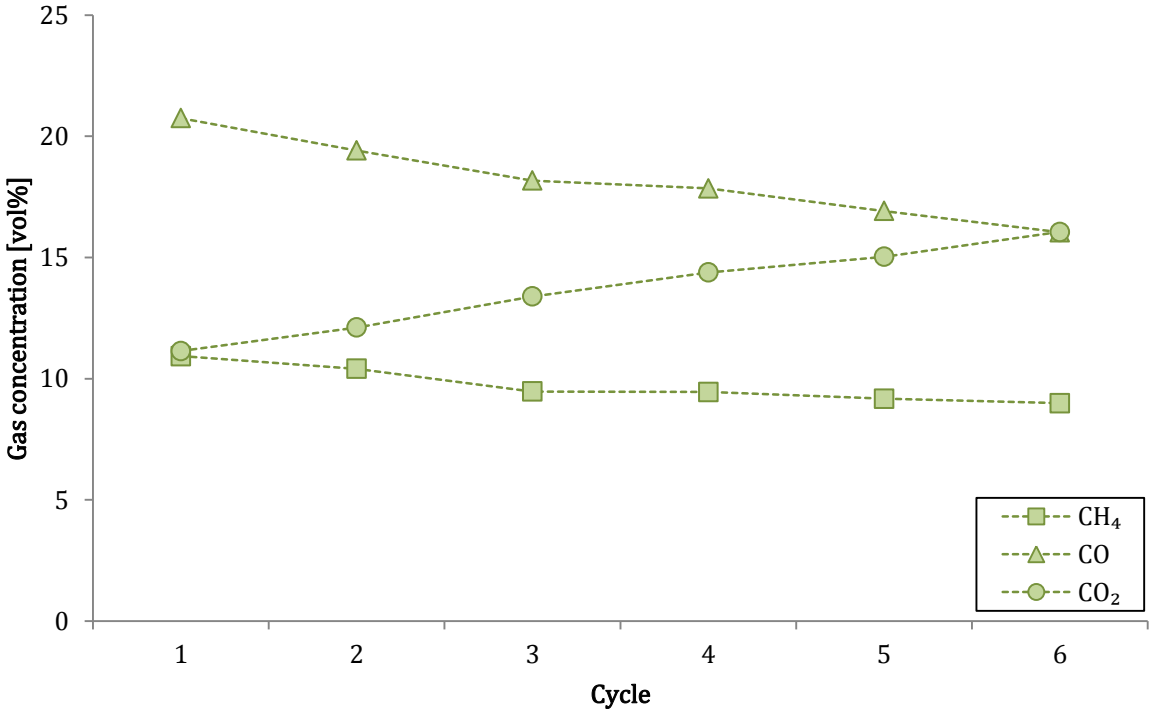

Figure 4-9. Product gas concentrations during gasification of a fuel mixture of 20 wt% wheat straw and 80 wt% forestry residues using olivine as bed material. Only a single experiment was performed.

For all three bed materials, the concentrations of CO and CH_4 gradually decreased over time while the concentration of CO_2 increased. As a result, the CO/CO_2 ratio decreased in all experiments as shown in Figure 4-10. When taking uncertainty into account, no significant differences in this quantity could be distinguished between the bed materials.

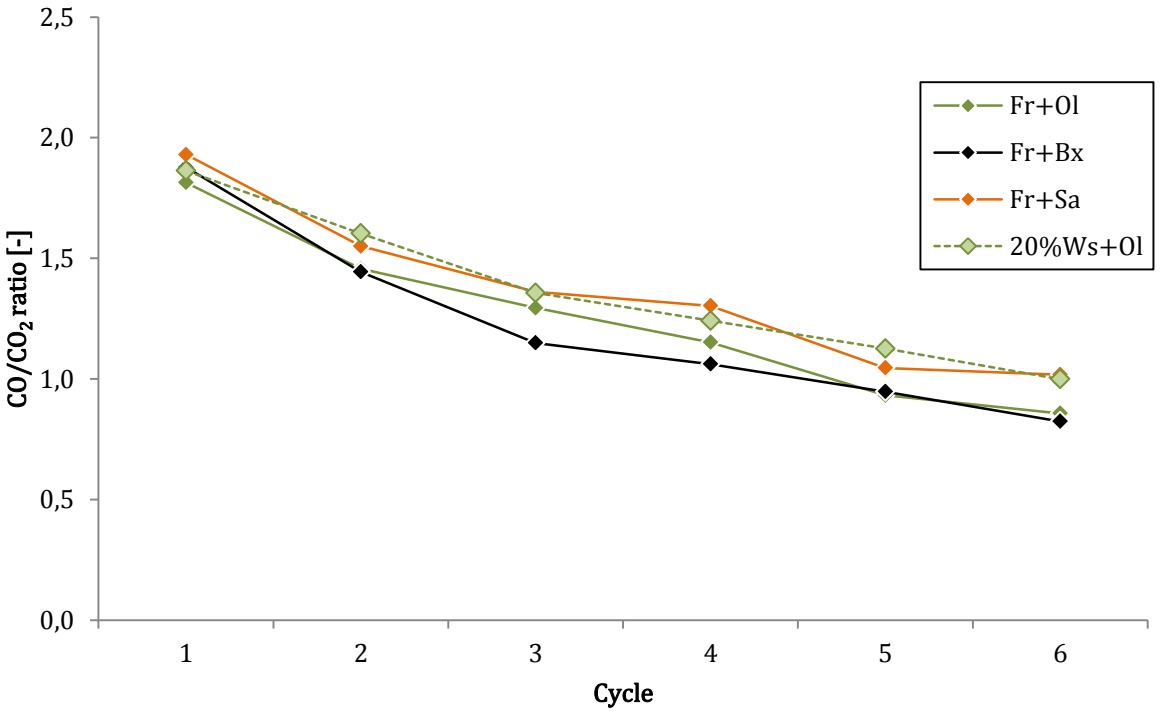

Figure 4-10. CO/CO_2 ratio of the product gas during gasification of forestry residues.

Regarding gas composition the difference between the bed materials was small, with the exception of sand where CO_2 production was slightly lower and CO and CH_4 concentrations were slightly higher. The average gas yields during gasification are presented in Figure 4-11.

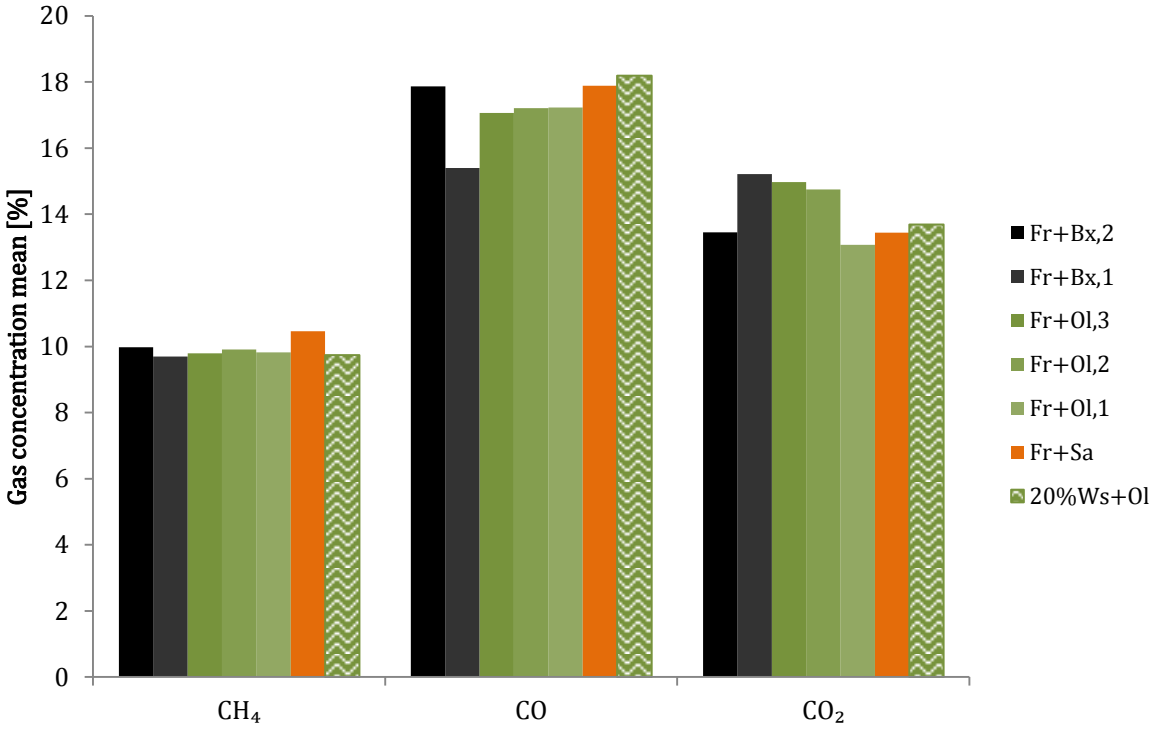

Figure 4-11. Average gas yields for the set *i* experiments.

5 Discussion

As presented in Section 4.1, the main ash-forming elements in the forestry residues that were retained on the surface of the three bed materials were P, Ca and K. As can be seen in the fuel analysis presented in in Figure 3-2, these elements were also among the five most abundant ash-forming elements in the forestry residues. It is therefore reasonable to conclude that the high extent of retention of these ash-forming elements was due to their abundance in the forestry residues. This conclusion is also in line with the fact that the outer layer of the bed materials were analyzed, and it has been shown in literature that the composition of the outer layer of used bed materials typically resembles that of the fuel ash (Grimm et al., 2012). However, even though the same amount of forestry residues (and therefore similar amounts of ash-forming elements) was thermally converted using each of the three bed materials (see set *i* experiments, described in Section 3.5), the extent of the retention of P, Ca and K on each of the three bed materials differed. For example, the retention of K from the forestry residue was higher on sand than that on olivine and bauxite. This indicates that the bed materials have certain intrinsic chemical and/or physical properties that influence their retention of ash-forming elements from biomass.

Under temperatures commonly applied in fluidized bed gasification and combustion processes, Si-rich bed materials favor the formation of potassium silicates when K-rich biomass fuels are fired (see Section 2.4.1.1). The higher concentration of Si in the sand compared to that of the olivine and bauxite (see Figure 3-4) thus explains why K was retained to a larger extent on sand than on bauxite or olivine. According to literature, Ca reacts with Si in bed materials to form calcium silicates, especially in the cases when the concentration of Ca is higher than that of the K in the fuel ash (Brus et al., 2005). While this may explain the higher retention of Ca on sand than olivine, the high retention of Ca on bauxite compared to that on olivine still lacks an explanation as the concentration of Si in the virgin bauxite was far lower than that in the virgin olivine. An explanation for this outcome will be sought in a planned future work, where the inner and outer layers of the used bed materials will be analyzed.

The retention of Ca, P and K was also influenced by the reactor atmosphere as presented in Section 4.2. P and Ca were retained on olivine primarily during char combustion as opposed to during gasification of the forestry residues. It might be tempting to conclude that this was solely a result of the char combustion lasting 3 times as long as the gasification of the forestry residues. However, K was retained to similar extents during both gasification of the forestry residues and combustion of the unconverted char. The discrepancy in the extents to which Ca, P and K were retained on olivine during thermal conversion of the forestry residues indicates that these elements possess certain intrinsic properties which enables them to be retained on the olivine under given atmospheres. According to previous studies on the release of ash-forming elements from biomass fuels, K is released during thermal conversion processes while Ca and P are mainly retained in the ash (Tchoffor et al., 2013, Zhang et al., 2012, Pedersen et al., 2010). Since most of the ash remains in the char during gasification, only a limited amount of Ca and P can be retained on the bed material during gasification. During char combustion, the organic matrix of the char is completely combusted which allows the residual ash to be deposited on the bed material. This explains why Ca and P were retained on the bed material mainly during the combustion stage. Although K is volatile at temperatures over 700 °C and therefore may be released during both gasification and combustion of biomass fuels, it has been observed in previous studies that K is mainly released from biomass during char combustion (Tchoffor et al., 2013, Knudsen et al., 2004). However, not all of the released K is retained on the bed material as a certain amount may leave the reactor with the product gas (during gasification) or flue gas (during combustion). This plausibly explains why the retention of K on the olivine was not higher during char combustion than during gasification of the forestry residues, as was the case for Ca and P.

The retention of ash-forming elements on the bed material particles may impact the thermal conversion process positively or negatively. From the set *iii* experiments (described in Section 3.5) in which wheat straw was thermally converted with each of the three bed materials, it was observed that sand was the least resistant to agglomeration while olivine was the most resistant. The difference in agglomeration tendency can be attributed to the propensity of ash-forming elements from the fuel to be

retained on the particle surfaces. Table 5-1 shows the molar ratios of (Si+P+K)/(Ca+Mg) on the outer layer of the bed materials which were sampled from the reactor after thermal conversion of forestry residues and wheat straw (or a mixture thereof). This ratio is indicative of the probability of ash melting and subsequent agglomeration to occur, where a higher ratio represents a higher probability. The results show that the experiments with wheat straw produced higher molar ratios for sand and bauxite, which suggests that these two bed materials were coated with molten ash material to a larger extent than olivine. This would explain why olivine was more resistant to agglomeration than sand and bauxite.

Table 5-1. Index ratios for the samples collected during the set *i* and *iii* experiments.

Bed material	Forestry residue experiment Unagglomerated samples	$\frac{Si+P+K}{Ca+Mg}$ Molar ratio Unagglomerated sample		$\frac{Si+P+K}{Ca+Mg}$ Molar ratio Agglomerated sample	Wheat straw experiment Agglomerated samples
Sand	Fr+Sa	27.1		212.3	Ws+Sa
Olivine	Fr+Ol,3	2.1		2.2	Ws+Ol
	Fr+Ol,2	2.0			
	Fr+Ol,1	2.1			
Olivine (fuel mix)*	20%Ws+Ol	2.2		2.1	33%Ws+Ol
Bauxite	Fr+Bx,2	4.8		54.8	Ws+Bx,2
	Fr+Bx,1	4.0		51.6	Ws+Bx,1

Although K is prone to cause agglomeration, it has been observed in previous studies that K may catalyze char and tar conversion. Therefore, a fuel with a low K content (e.g. forestry residues) may limit char and tar conversion. It may then be desirable to increase the K content of a fuel, but not to an extent which approaches that of common K-rich fuels (e.g. wheat straw) since a high fuel content of K is associated with a high risk of agglomeration. A way to achieve this is to mix a K-lean fuel with a K-rich fuel. An experiment carried out with a mixture of forestry residue and straw consisting of 20 wt% straw under similar conditions as an experiment carried out with only forestry residues did not result in agglomeration. If a higher fuel K content it is desired, the results suggest that it may be possible to blend small amounts of wheat straw (e.g. 5 wt%) into a forestry residues/wheat straw fuel mix to be used in DFBG.

The extents of the retention of K, Ca and P on the bed materials had a marginal effect on the concentrations of CO, CO_2 and CH_4 in the product gas during gasification of the forestry residues. According to literature (see Section 2.4.2.2), the retention of Ca on bed materials catalyzes the water-gas shift reaction. The CO/CO_2 ratio can give an indication of the extent of water-gas shift occurring during gasification (Simonetti, 2008). In the present work, Ca was retained to a larger extent on bauxite (and sand) than on olivine during thermal conversion of forestry residues. However, the CO/CO_2 ratio in the product gas was similar for all three bed materials which indicates that the degree of water-gas shift catalysis was similar for the three bed materials (see Figure 4-10).

6 Conclusions

The main aim of this work was to investigate the propensity of bed materials to retain ash-forming elements from biomass under conditions relevant to DFBG. In addition, the effect of the retention of ash-forming elements on the composition of the product gas and the resistance of the bed materials to be agglomerated was investigated.

The investigation was carried out in the temperature range 800–900 °C. Three bed materials were studied: sand, olivine and bauxite. The propensity of these bed materials to retain ash-forming elements from biomass fuels was studied with forestry residues and a mixture of wheat straw and forestry residues consisting of 20 wt% wheat straw. In order to determine the resistance of the bed materials to be agglomerated within the investigated temperature range, a long operation time would have been needed owing to the low ash content of the forestry residues. Since the fluidized bed reactor

used in the present work could only be operated for a limited length of time during each experiment, a biomass fuel of higher ash content (wheat straw) was used to assess the resistance of the bed materials to be agglomerated.

Based on the results from the experiments and literature on ash transformation during thermal conversion of biomass, the following conclusions were drawn:

1) During dual fluidized bed gasification of biomass using sand, olivine and bauxite, the ash-forming elements that are retained to the largest extent on the bed materials are those that are most abundant in the biomass. However, ash-forming elements are retained to different extents on different bed materials. During thermal conversion of biomass with a composition similar to the forestry residues studied in the present work, it is likely that Ca, P and K are the ash-forming elements retained to the largest extent on the bed materials. The extent of retention of P on the bed materials is likely to follow the order of bauxite > (sand ≈ olivine). The retention of Ca is likely to follow the order of (bauxite ≈ sand) > olivine. The retention of K is likely to follow the order of sand > (bauxite ≈ olivine). The difference in the extents to which the ash-forming elements are retained on the bed materials is plausibly related to their respective tendency to form compounds.
2) The retention of ash-forming elements on bed materials during DFBG is influenced by the atmosphere surrounding the fuel particles in the reactor. Non-volatile ash-forming elements like Ca and P are more likely to be retained on the bed material during the char combustion stage than during the gasification stage. Contrary to Ca and K, volatile ash-forming elements like K can be retained to similar extents during the gasification and char combustion stages.
3) If a biomass fuel with a high ash content and/or a high K content is to be thermally converted with sand, olivine or bauxite under conditions relevant to DFBG, the resistance of the bed materials to be agglomerated will follow the order of olivine ≫ bauxite > sand. This trend was found to correlate with the molar ratio of (Si+P+K)/(Ca+Mg) on the outer layers of the bed material samples. According to literature, the higher this ratio, the more likely agglomeration is to occur. This ratio followed the order of (sand > bauxite) ≫ olivine.

   If it is desired to increase the presence of K in an olivine DFBG system, the high agglomeration resistance of olivine suggests it may be possible to use a fuel mixture where a small amount of a K-rich fuel (e.g. wheat straw) is mixed with a K-lean fuel while maintaining a low risk of agglomeration.
4) No significant difference in the concentrations of CO, CO_2 and CH_4 in the product gas can be expected upon gasification of forestry residues when sand, bauxite or olivine is used in a DFBG process. While the retention of Ca differs between bed materials and it has been suggested in literature that retained Ca catalyzes the water-gas shift reaction, a marginal difference in the CO/CO_2 ratio in the product gas was observed in the present work when forestry residues were gasified using each of the bed materials.

In summary, if a choice is to be made among the bed materials sand, bauxite and olivine for suitability in a DFBG process in terms of degree of water-gas shift catalysis and risk of agglomeration, the results suggest that sand (being the cheapest of the three bed materials) can be used if the fuel is virtually free of contaminants and of low ash content. Its usage should pose no additional risk of agglomeration under these circumstances. However, if the fuel is of a higher ash content and/or contains K to a large extent, olivine is considerably more resistant to agglomeration which may favor its usage. It is also important to mention that there are other effects on the DFBG process that can be attributed to the retention of ash-forming elements which should be considered when selecting a suitable bed material. For example, the ability of a bed material to catalyze tar conversion may be of importance.

7 Future work

In the present work, the bed materials used during thermal conversion of biomass were analyzed with XRF in order to determine the elemental composition of the outer layer of the retained ash-forming elements. In a planned future work the inner layer of the retained ash-forming elements will be analyzed with SEM-EDX (*Scanning electron microscopy with energy-dispersive x-ray spectroscopy*). In addition, XRD (*X-ray diffraction*) analysis of the outer layer will be undertaken in order to determine in what chemical form the ash-forming elements are present on the bed material particle. In order to better understand the connection between retention of ash-forming elements and breakdown of tars, it may be desired to investigate differences in tar yield during thermal conversion of biomass in fluidized bed reactors operated with different bed materials. In addition, it may be valuable to measure the concentration of H_2 in the product gas during gasification of biomass in fluidized beds in order to better understand the effect of the retained ash-forming elements regarding e.g. catalysis of the water-gas shift reaction.

8 List of references

ABU EL-RUB, Z., BRAMER, E. & BREM, G. 2004. Review of catalysts for tar elimination in biomass gasification processes. *Industrial & Engineering Chemistry Research,* 43**,** 6911-6919.

AHO, M. & SILVENNOINEN, J. 2004. Preventing chlorine deposition on heat transfer surfaces with aluminium–silicon rich biomass residue and additive. *Fuel,* 83**,** 1299-1305.

AHRENFELDT, J., THOMSEN, T. P., HENRIKSEN, U. & CLAUSEN, L. R. 2013. Biomass gasification cogeneration – A review of state of the art technology and near future perspectives. *Applied Thermal Engineering,* 50**,** 1407-1417.

ALVAREZ, H. 2006. *Energiteknik,* Studentlitteratur AB.

ANKARSMID SAMPLING 2010. *User Manual Portable Gas Conditioning System Series APS 30x, 31x with O2 measurement ASP 100/ASP101*.

BASU, P. 2006. *Combustion and gasification in fluidized beds*, CRC press.

BASU, P. 2010. *Biomass gasification and pyrolysis: practical design and theory*, Academic press.

BP 2013. BP Statistical Review of World Energy June 2013. BP.

BRUS, E., ÖHMAN, M. & NORDIN, A. 2005. Mechanisms of bed agglomeration during fluidized-bed combustion of biomass fuels. *Energy & Fuels,* 19**,** 825-832.

CORELLA, J., TOLEDO, J. M. & MOLINA, G. 2007. A review on dual fluidized-bed biomass gasifiers. *Industrial & Engineering Chemistry Research,* 46**,** 6831-6839.

DAYTON, D. & MILNE, T. 1995. Mechanisms of alkali metal release during biomass combustion. *Preprints of Papers, American Chemical Society, Division of Fuel Chemistry,* 40.

DE GEYTER, S., ÖHMAN, M., BOSTRÖM, D., ERIKSSON, M. & NORDIN, A. 2007. Effects of non-quartz minerals in natural bed sand on agglomeration characteristics during fluidized bed combustion of biomass fuels. *Energy & fuels,* 21**,** 2663-2668.

FRYDA, L. E., PANOPOULOS, K. D. & KAKARAS, E. 2008. Agglomeration in fluidised bed gasification of biomass. *Powder Technology,* 181**,** 307-320.

GELDART, D. 1973. Types of gas fluidization. *Powder Technology,* 7**,** 285-292.

GRACE, J. 1982. Fluidized bed hydrodynamics. *Handbook of multiphase systems,* 5.

GRIMM, A., SKOGLUND, N., BOSTRÖM, D., BOMAN, C. & ÖHMAN, M. 2012. Influence of phosphorus on alkali distribution during combustion of logging residues and wheat straw in a bench-scale fluidized bed. *Energy & Fuels,* 26**,** 3012-3023.

JENKINS, B., BAXTER, L., MILES JR, T. & MILES, T. 1998. Combustion properties of biomass. *Fuel Processing Technology,* 54**,** 17-46.

KIRNBAUER, F., WILK, V. & HOFBAUER, H. 2013. Performance improvement of dual fluidized bed gasifiers by temperature reduction: The behavior of tar species in the product gas. *Fuel,* 108**,** 534-542.

KIRNBAUER, F., WILK, V., KITZLER, H., KERN, S. & HOFBAUER, H. 2012. The positive effects of bed material coating on tar reduction in a dual fluidized bed gasifier. *Fuel,* 95**,** 553-562.

KNUDSEN, J. N., JENSEN, P. A. & DAM-JOHANSEN, K. 2004. Transformation and release to the gas phase of Cl, K, and S during combustion of annual biomass. *Energy & Fuels,* 18**,** 1385-1399.

KRAMAR, U. 1997. Advances in energy-dispersive X-ray fluorescence. *Journal of Geochemical Exploration,* 58**,** 73-80.

KUO, J.-H., WEY, M.-Y., LIN, C.-L. & CHIU, H.-M. 2008. The effect of aluminum inhibition on the defluidization behavior and generation of pollutants in fluidized bed incineration. *Fuel Processing Technology,* 89**,** 1227-1236.

LARSSON, A., SEEMANN, M., NEVES, D. & THUNMAN, H. 2013. Evaluation of performance of industrial-scale dual fluidized bed gasifiers using the chalmers 2–4-MWth gasifier. *Energy & Fuels,* 27**,** 6665-6680.

LEHTIKANGAS, P. 1998. *Lagringshandbok för trädbränslen*, Institutionen för virkeslära, SLU Uppsala.

LIN, W., DAM-JOHANSEN, K. & FRANDSEN, F. 2003. Agglomeration in bio-fuel fired fluidized bed combustors. *Chemical Engineering Journal,* 96**,** 171-185.

LV, P. M., XIONG, Z. H., CHANG, J., WU, C. Z., CHEN, Y. & ZHU, J. X. 2004. An experimental study on biomass air–steam gasification in a fluidized bed. *Bioresource Technology,* 95**,** 95-101.

M.W. CHASE JR, C. A. D., J.R. DAVIES JR, D.J.FULRIP, R.A. MCDONALD, A.N. SYVERUD 1985. JANAF Thermochemical Tables, Third Edition. *Journal of Physical and Chemical Reference Data*.

MASTELLONE, M. L. & ARENA, U. 2008. Olivine as a tar removal catalyst during fluidized bed gasification of plastic waste. *AIChE Journal,* 54**,** 1656-1667.

MCKENDRY, P. 2002. Energy production from biomass (part 1): overview of biomass. *Bioresource Technology,* 83**,** 37-46.

MILES, T. R., MILES JR, T. R., BAXTER, L. L., BRYERS, R. W., JENKINS, B. M. & ODEN, L. L. 1996. Boiler deposits from firing biomass fuels. *Biomass and Bioenergy,* 10**,** 125-138.

NORDLING, C. & ÖSTERMAN, J. 2004. *Physics handbook for science and engineering*, Studentlitteratur.

OJHA, R., MENON, N. & DURIAN, D. 2000. Hysteresis and packing in gas-fluidized beds. *Physical Review E,* 62**,** 4442.

PEDERSEN, A. J., VAN LITH, S. C., FRANDSEN, F. J., STEINSEN, S. D. & HOLGERSEN, L. B. 2010. Release to the gas phase of metals, S and Cl during combustion of dedicated waste fractions. *Fuel Processing Technology,* 91**,** 1062-1072.

PFEIFER, C., KOPPATZ, S. & HOFBAUER, H. 2011. Steam gasification of various feedstocks at a dual fluidised bed gasifier: Impacts of operation conditions and bed materials. *Biomass Conversion and Biorefinery,* 1**,** 39-53.

RAPAGNA, S., JAND, N., KIENNEMANN, A. & FOSCOLO, P. 2000. Steam-gasification of biomass in a fluidised-bed of olivine particles. *Biomass and Bioenergy,* 19**,** 187-197.

RAUCH, R., HOFBAUER, H., BOSCH, K., SIEFERT, I., AICHERNIG, C., TREMMEL, H., VOIGTLAENDER, K., KOCH, R. & LEHNER, R. Steam gasification of biomass at CHP plant Guessing-Status of the demonstration plant. 2nd world conference and technology exhibition on biomass for energy, industry and climate protection, Rome, Italy, 2004.

ROSEMOUNT ANALYTICAL 1997. *Operation Manual Binos 100 NDIR-Analyzer*.

ROY, G. & SARMA, K. 1970. Fluidized bed heat transfer. *Chemical Processing*.

SAIDUR, R., ABDELAZIZ, E., DEMIRBAS, A., HOSSAIN, M. & MEKHILEF, S. 2011. A review on biomass as a fuel for boilers. *Renewable and Sustainable Energy Reviews,* 15**,** 2262-2289.

SIMONETTI, D. A. 2008. *The production of liquid fuels and chemicals from biomass derived polyols by catalytic coupling*, ProQuest.

SKRIFVARS, B.-J., HUPA, M., BACKMAN, R. & HILTUNEN, M. 1994. Sintering mechanisms of FBC ashes. *Fuel,* 73**,** 171-176.

SOMMERSACHER, P., BRUNNER, T. & OBERNBERGER, I. 2011. Fuel indexes: A novel method for the evaluation of relevant combustion properties of new biomass fuels. *Energy & Fuels,* 26**,** 380-390.

STRÖMBERG, B. & SVÄRD, S. H. 2012. *Bränslehandboken 2012,* Stockholm.

SUTHERLAND, W. 1893. LII. The viscosity of gases and molecular force. *The London, Edinburgh, and Dublin Philosophical Magazine and Journal of Science,* 36**,** 507-531.

TCHOFFOR, P. A., DAVIDSSON, K. O. & THUNMAN, H. 2013. Transformation and release of potassium, chlorine, and sulfur from wheat straw under conditions relevant to dual fluidized bed gasification. *Energy & fuels,* 27**,** 7510-7520.

WERKELIN, J., SKRIFVARS, B.-J. & HUPA, M. 2005. Ash-forming elements in four Scandinavian wood species. Part 1: Summer harvest. *Biomass and Bioenergy,* 29**,** 451-466.

WERTHER, J., SAENGER, M., HARTGE, E.-U., OGADA, T. & SIAGI, Z. 2000. Combustion of agricultural residues. *Progress in energy and combustion science,* 26**,** 1-27.

VISSER, H. J. M. 2004. *The influence of fuel composition on agglomeration behaviour in fluidised-bed combustion*, Energy research Centre of the Netherlands ECN.

WOLF, K., MÜLLER, M., HILPERT, K. & SINGHEISER, L. 2004. Alkali sorption in second-generation pressurized fluidized-bed combustion. *Energy & fuels,* 18**,** 1841-1850.

VUTHALURU, H. B., LINJEWILE, T. M., ZHANG, D.-K. & MANZOORI, A. R. 1999. Investigations into the control of agglomeration and defluidisation during fluidised-bed combustion of low-rank coals. *Fuel,* 78**,** 419-425.

XU, G., MURAKAMI, T., SUDA, T., MATSUZAWA, Y. & TANI, H. 2006. Gasification of coffee grounds in dual fluidized bed: performance evaluation and parametric investigation. *Energy & fuels,* 20**,** 2695-2704.

YANG, W.-C. 2003. *Handbook of fluidization and fluid-particle systems,* CRC Press.

ZHANG, Z.-H., SONG, Q., YAO, Q. & YANG, R.-M. 2012. Influence of the atmosphere on the transformation of alkali and alkaline earth metallic species during rice straw thermal conversion. *Energy & Fuels,* 26**,** 1892-1899.

Appendix A. Fuel preparation and feeding

Prior to each experiment, the pellets were dried to constant mass in an oven where the temperature was held at 105 °C for at least 8 hours. In order to ensure a constant fuel feeding rate during the experiments, the dried pellets were sorted into 3 weight fractions: $0.55\ g \leq m < 0.65\ g$, $0.65\ g \leq m < 0.75\ g$ and $0.75\ g \leq m < 0.85\ g$. No pellet in a fraction had a weight deviating more than 0.05 g from the mean, which was assumed to lie in the middle of the weight span. In order to maintain a constant fuel mass flow in the different experiments the frequency of fuel feeding was altered depending on fuel weight fraction. Fuel feeding was performed manually. See Appendix Table A-1.

Appendix Table A-1. Fuel feeding intervals used to obtained constant mass flow across fuel weight fractions.

Average fuel pellet weight [g]	Pellets per second [pcs/s]	Fuel mass flow [g/min]
0.60	0.32	11.56
0.70	0.28	
0.80	0.24	

Appendix B. Physical properties of bed materials

B.1 Size distribution

Primary bed material fractioning was performed for all bed materials using a rotating sieve shaker to remove fractions larger than or equal of 500 µm and smaller than 250 µm. The sieve shaker was operated at 200 RPM for 2 minutes. Secondary bed material fractioning of the material was thereafter performed through additional mechanical or manual sieving. This was conducted in order to ensure no unreasonable amounts of undersizes (< 250 µm) remained. The fractioned materials were thereafter evaluated through sieve analysis.

The particle size distribution of the fractioned material was determined through sieve analysis where a stack of sieves of mesh aperture sizes 1000, 500, 355, 250, 180 and 75 µm were used. A small amount[2] of randomly sampled bed material was sieved manually for one minute. The retained weight on each sieve was noted and the percent passing was calculated and plotted. In Appendix Figure B-1, particle size distributions for the bed materials used are presented. As each sieve analysis was performed in duplex, the mean value is presented for each bed material.

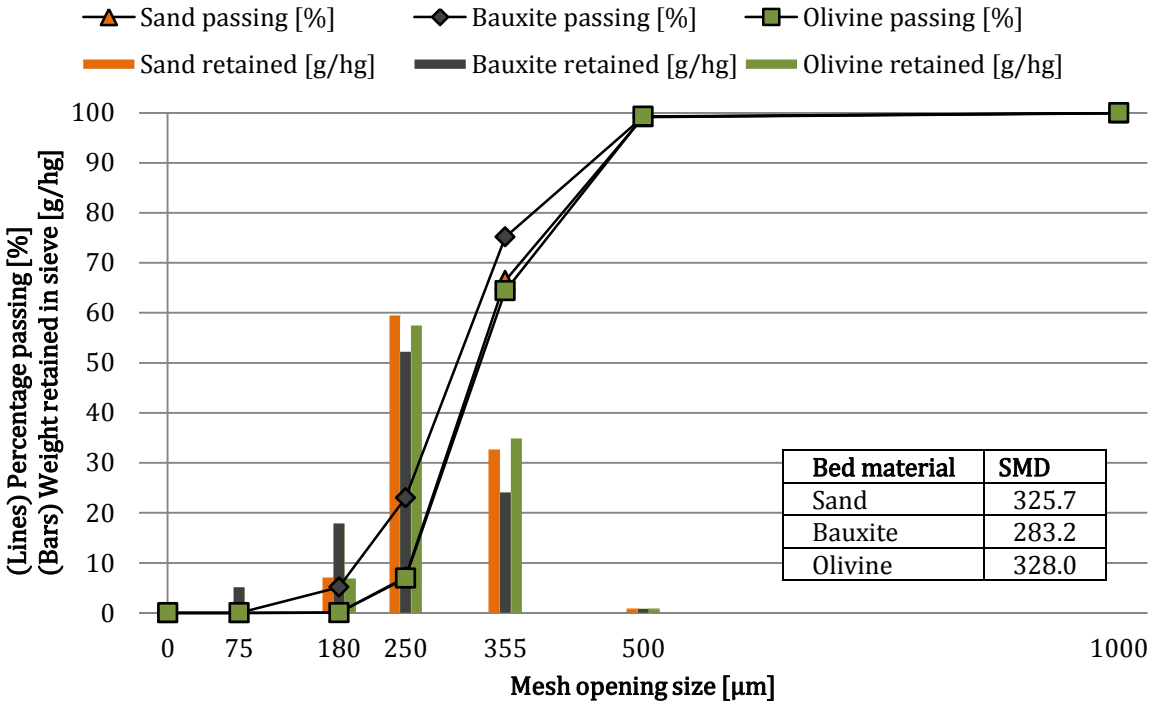

Appendix Figure B-1. Sieve analysis of the fractioned bed materials of target diameter 250 ≤ d < 500 µm.

Based on the sieve analyses of the bed materials, the SMD was calculated as presented in the table inset of Appendix Figure B-1.

Through sieve analysis of the samples it was determined that no presence of particles smaller than 180 µm could be detected with the equipment available in the case of olivine and sand. However, the bauxite did contain a certain amount of small particles after fractioning: the content of particles of 75 µm or larger was close to 5 %, but no amount of particles smaller than 75 µm could be detected. The bauxite was determined to be feasible for study in this regard despite the presence of particles in the 75 µm range. The implications of this are discussed in Appendix F.4.

Notable dusting was observed upon handling of all fractioned bed materials which was indicative of a continued presence of smaller particles even after fractioning. Judging from the precision of the scales

[2] Samples in the range of 70–130 g.

used, an estimation of potential content of particles of size < 75 µm is that this fraction should not constitute more than 0.1 % of the mass of the total bed material for any of the bed materials studied. As it would demand numerous repeated sieving runs with smaller batch sizes and longer agitation periods to remove all particles of size < 250 µm, a certain amount of undersizes were allowed to remain in the bed material.

Besides the practical difficulties involved, the arguments for this decision were two. Firstly, the particle size distributions in the relevant size range was relatively similar across the bed materials. It is worth noting that most studies use raw bed material where little attention is paid to bed material particle size distribution on this level of detail. In this regard, the sieved bed materials studied here can be regarded as similar despite the smaller fraction remaining in the bauxite. Secondly, no substantial amount of particles small enough to be entrained out of the bed were believed to be prevalent, as the sieve analysis indicated. The fractioning was therefore considered sufficient and all bed materials were deemed to be feasible for study in this aspect.

B.2 Particle density

The particle density of the bed materials is relevant to the calculation of U_{mf} and U_t. As only simple equipment was available, particle density was measured with approximate methods. A weighed amount of bed material was introduced into a 100-ml volumetric flask, which was then filled to the mark using a measured amount of water from a 100-ml graduated cylinder. When the volumetric flask was filled to the mark, the volume occupied by the bed material was then approximately equal to the residual amount of water present in the graduated cylinder. Using this method, the particle density was approximated to 2,700 and 3,300 kg/m^3 for sand and olivine, respectively.

It is worth noting that the particle density should be equal for a given material irrespective of its particle size distribution. Particle density determination of a bed material, one finely ground and one coarsely ground, was carried out in order to indicate the magnitude of the experimental error. The difference was found to be close to 300 kg/m^3. While residual air bubbles in the material is one probable cause of error, a more likely source of error is the reading of the graduated cylinder, which was graduated and read in steps of 1 ml. Sensitivity analysis showed that a misreading of ½ ml can result in a particle density value differing close to 250 kg/m^3 under these circumstances. The calculated particle densities of bed materials should therefore be regarded as a coarse approximation.

B.3 Moisture content

The moisture content of all bed materials was determined by heating bed material samples 105 °C in an oven where temperatures were kept constant for 24 hours. After drying, the weight difference was calculated. With the scales used, no moisture content could be detected for any of the bed materials. Based on these results, the bed materials used in the experiments were not dried prior to usage and the influence of bed material moisture content was neglected.

Appendix C. Lab analysis results

Appendix Table C-1. Lab analysis results for fuels and bed materials.

On sample in state of submission	Straw	Forestry residue	Bauxite	Olivine	Silica sand
Total moisture, wt%	10.4	11.8	-	-	-
Ash, wt%	3.9	1.5	-	-	-
Chlorine, Cl, wt%	0.17	0.01	-	-	-
Sulfur, S, wt%	0.07	0.03	-	-	-
Carbon, C, wt%	42	44.4	-	-	-
Hydrogen, H, wt%	6.4	6.7	-	-	-
Nitrogen, N, wt%	0.62	0.44	-	-	-
Higher heating value at constant volume, MJ/kg	16.97	17.86	-	-	-
Lower heating value at constant pressure, MJ/kg	15.57	16.39	-	-	-
On dried sample	**Straw**	**Forestry residue**	**Bauxite**	**Olivine**	**Silica sand**
Ash, wt%	4.3	1.8	-	-	-
Chlorine, Cl, wt%	0.2	0.01	-	-	-
Leachable chloride, Cl-, wt%	-	-	<0.01	0.01	<0.01
Sulfur, S, wt%	0.07	0.03	0.02	0.02	0.01
Carbon, C, wt%	46.8	50.3	-	-	-
Hydrogen, H, wt%	5.8	6.1	-	-	-
Nitrogen, N, wt%	0.69	0.5	-	-	-
Oxygen, O, (diff) wt%	42	41	-	-	-
Aluminium, Al, wt%	0.032	0.021	47.7	0.15	2.66
Silica, Si, wt%	0.87	0.12	4.07	19.8	45
Iron, Fe, wt%	0.042	0.026	1.07	5.4	0.34
Titanium, Ti, wt%	0.002	0.001	1.77	0.07	0.07
Manganese, Mn, wt%	0.003	0.021	<0.05	0.08	0.01
Magnesium, Mg, wt%	0.097	0.053	0.05	32.4	0.06
Calcium, Ca, wt%	0.30	0.43	0.15	0.05	0.31
Barium, Ba, wt%	0.003	0.006	<0.05	<0.05	<0.05
Sodium, Na, wt%	0.045	0.013	<0.1	0.06	0.93
Potassium, K, wt%	0.96	0.19	0.19	0.16	1.78
Phosphorus, P, wt%	0.07	0.04	<0.1	<0.1	<0.1
Higher heating value at constant volume, MJ/kg	18.93	20.24	-	-	-
Lower heating value at constant pressure, MJ/kg	17.66	18.91	-	-	-

Appendix Table C-2. Lab analysis results of thermally treated fuels.

On sample after ashing at 550 °C	**Straw**	**Forestry residue**
Aluminium, Al, wt%	0.73	1.15
Silica, Si, wt%	20.2	6.73
Iron, Fe, wt%	0.97	1.38
Titanium, Ti, wt%	0.04	0.06
Manganese, Mn, wt%	0.06	1.16
Magnesium, Mg, wt%	2.25	2.87
Calcium, Ca, wt%	6.91	23.3
Barium, Ba, wt%	0.07	0.34
Sodium, Na, wt%	1.03	0.73
Phosphorus, P, wt%	1.69	2.01

Appendix Table C-3. Measurement methods of the lab analysis.

Element	*Method of measurement*
Fe	Mod. ASTM D 3682
Mn	Mod. ASTM D 3682
Ti	Mod. ASTM D 3682
Al	Mod. ASTM D 3682
S	SS-EN 15289
P	Mod. ASTM D 3682
Si	Mod. ASTM D 3682
Mg	Mod. ASTM D 3682
Ba	Mod. ASTM D 3682
Ca	Mod. ASTM D 3682
K	Microwave digestion and ICP-OES
Cl	Leaching and ion chromatography
Na	Mod. ASTM D 3682

Appendix D. Principles of measurement

The gases studied were CO, CO_2, and CH_4. These gases have major roles in combustion and gasification reactions as outlined in Sections 2.3.1 and 2.3.2. While measurement of H_2 would be desirable no measurement of this gas was undertaken due to unavailability of instruments.

Measurement of product gas composition was conducted with NDIR instruments. These rely on difference in absorption of infrared light between gases to determine gas concentrations. The absorbed wavelength is a characteristic of the gas and the strength of absorption is indicative of gas concentration (Rosemount Analytical, 1997).

For the on-line measurement of O_2 paramagnetic measurement was used. The measuring principle is based on that oxygen, unlike many other gases, is attracted to magnetic fields. Owing to the attraction of O_2 to magnetic fields, a sensor placed in a magnetic field is displaced when exposed to an oxygen-containing gas. Through measuring this displacement through optical and electrical means, the concentration of O_2 in the gas can be determined (Ankarsmid Sampling, 2010).

For analysis of bed material surfaces XRF analysis was used. It is a non-destructive surface analysis method based on x-ray excitation of electrons in materials: when an excited electron returns to the normal state, radiation is emitted that is characteristic for the element (Kramar, 1997).

Appendix E. Operating parameters

The target operating parameters are presented in Appendix Table E-1. These were taken in order to be representative of commercial biomass FB gasifiers. However, nitrogen was added both in the gasification and combustion stage in order to maintain concentrations of measured gases within the range of sensitivity of the instruments. The appropriate nitrogen flows for this purpose was determined experimentally during pre-trials. It was considered that the presence of nitrogen did not influence the chemistry of reactions significantly.

Appendix Table E-1. Target operating parameters for one experiment cycle.

	Gasification	Combustion
Steam-to-biomass ratio (mass)	0.9	0
Fuel feeding rate	11.56 g/min	0
Water flow	10.4 ml/min (l)	0
Temperature	860 °C (start)–800°C (end)	900 °C (peak)
Steam concentration [wt%]	65 %	0 %
Oxygen concentration [vol%]	0 %	6 %[3]
Nitrogen concentration [wt%]	35 %	94 %
Time period	4 minutes	12 minutes
Nitrogen flow	4.82 l/min	9.86 l/min
Air flow	0	3.94 l/min

Due to the relatively small amount of bed material present in the reactor, the introduction of fuel caused the reactor temperature to drop. This was primarily due to the endothermic reactions involved in gasification of the fuel. While the reactor was electrically heated, the temperature dropped at a rate faster than what could be compensated for. In most cases, temperatures reached around 800 °C at the end of the gasification period. Similarly, most combustion stages were undertaken with temperatures reaching close to 900 °C. However, these temperatures are in the range of normal operational parameters applied in industrial DFBG systems as presented in Section 2.3.3.

In Appendix Figure E-1, the maximum temperature of the cycle with the highest combustion temperature is presented as well as the lowest temperature of the cycle with the lowest gasification temperature. The temperatures of the 5 less extreme cycles in the set *i* experiments are not presented.

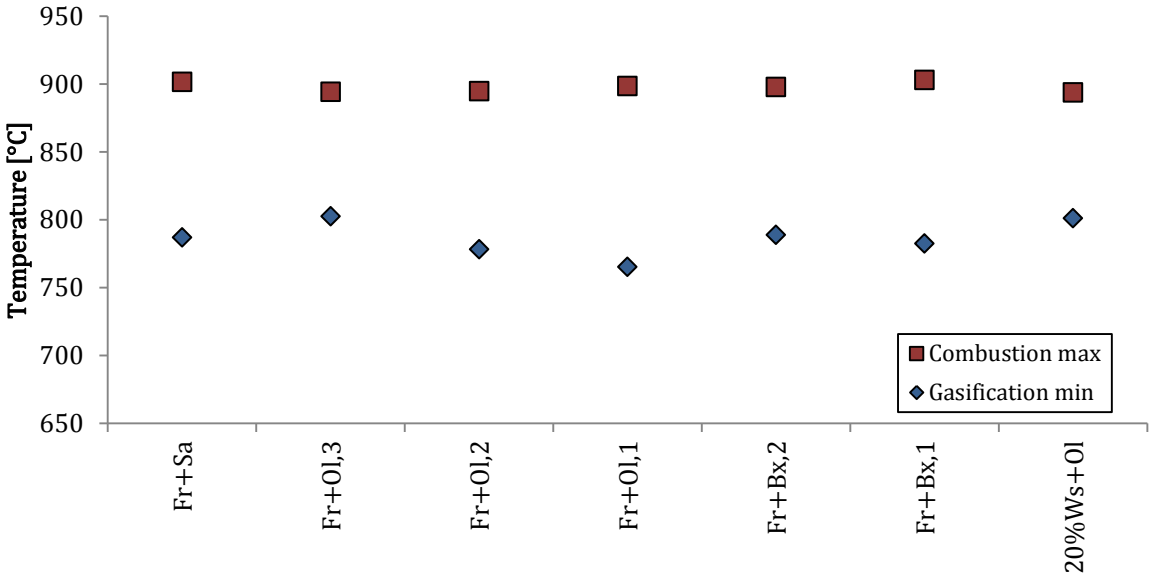

Appendix Figure E-1. Maximum temperatures of combustion periods and minimum temperatures of gasification periods during the set *i* experiments. Note that the temperatures axis is broken.

[3] The air feeding system lowered the oxygen concentration in air to approximately 19.5 %, which resulted in a slightly lower oxygen concentration (around 5,6 vol%) during combustion.

Appendix F. Hydrodynamic calculations

In order to be able to perform calculations of minimum fluidization velocity U_{mf} and terminal velocity U_t in a flexible manner, a spreadsheet model was developed. These quantities were calculated using the equations listed in Sections 2.2.1.1 and 2.2.1.2, as was the corresponding air volume flows to the reactor.

F.1 Dynamic or absolute viscosity of air

As suggested by (2.4, the dynamic or absolute viscosity μ of air can be calculated using a reference value of dynamic viscosity at a known temperature. However, the usage of the equation also involves using Sutherland's constant for air, here denoted S. Since a reliable source of it proved difficult to find in literature, literature values for the dynamic viscosity were used instead of (2.4. Values were taken from a data series of dynamic viscosities of air in the temperature range of 100 to 1 600 K (Basu, 2010). The tabulated range was considered sufficiently large to not limit the validity of the following calculations outside of practically realistic bounds. Values from the data series were interpolated using a third-degree polynomial curve fit.

F.2 Gas density

The gas density was calculated from the ideal gas law:

$$\rho_g = \frac{pM}{RT}$$

Appendix Equation D-1

The gas density is dependent on the temperature and pressure of the fluidization medium. The temperature is a variable, but the pressure is assumed to be constant and atmospheric. The molar mass of the gas is dependent on the gas composition. For atmospheric air[4], the simplification was made that air has four constituents in proportions according to Appendix Table F-1.

Appendix Table F-1. Atmospheric gas composition (Basu, 2010).

Atmospheric air composition	
Gas	*Share by volume [%]*
N_2	78.09 %
O_2	20.95 %
Ar	0.933 %
CO_2	0.03 %

The value of the molar gas constant R was taken from Nordling and Österman (2004) where $R = 8.314472\ J/kmol$.

F.3 Calculation results

The fluidization and terminal velocities are both dependent on temperature and bed material properties. Therefore, for each combination of temperature and bed material a specific set of fluidization and terminal velocities is valid. The results of the calculation for sand in pure steam are presented here along with values of corresponding volume flows.

[4] The calculation results presented are based on gasification in a pure steam environment, but the developed model was used for calculations of U_{mf} and U_t during combustion (in atmospheric air) as well.

Appendix Table F-2. Input and calculation of minimum fluidization velocity.

Input					
Symbol	**Physical quantity**	**Value**			**Source**
T	Temperature [°C]	**800**	**850**	**900**	Chosen
$d_{p,sand}$	mean particle diameter [µm]	325.7			Measured (Sand)
ρ_p	bed material density [kg/m³]	2727			Measured (Sand)
p	Air pressure [kPa]	101.3			Chosen (1 atm)
d	Reactor diameter [mm]	70.0			Measured
C_1	Empirical constant 1 for (2.2 (for Re_{mf})	27.2			(Grace, 1982)
C_2	Empirical constant 2 for (2.2 (for Re_{mf})	0.0408			(Grace, 1982)
µ	Absolute/dynamic viscosity of air [N s/m²]	4.4206E-05	4.5458E-05	4.6710E-05	(Basu, 2010)[5]
Calculation result					
Symbol	**Physical quantity**	**Value**			**Source**
T	Temperature [°C]	**800**	**850**	**900**	Chosen
ρ_g	gas density [kg/m³]	0.205	0.195	0.187	Calculated
Ar	Archimedes number [-]	114.8	100.6	88.9	Calculated
Re_{mf}	Reynolds number at minimum fluidization velocity [-]	0.086	0.075	0.067	Calculated
U_{mf}	Minimum fluidization velocity [m/s]	0.052	0.050	0.048	Calculated
Q_{mf}	air volume flow at U_{mf} [l/min]	12.1	11.6	11.1	Calculated
U_t	Terminal velocity	3.75	3.75	3.76	Calculated
Q_t	air volume flow at U_t [l/min]	865.5	866.3	867.4	Calculated

F.4 U_{mf}, U_t and particle entrainment

The calculations of minimum and ultimate fluidization velocity are based on a series of assumptions, such as that the gasification medium used is pure steam and that only sand is used. It can be argued that such assumptions are associated with uncertainties. However, the values of minimum and ultimate fluidization velocity are only used to define the limits of reactor operation: gas flows during gasification in the experiments were no more than 6 times greater than the calculated U_{mf} and never above 7 % of the calculated U_t. Since the U_t defines the upper limit of operation above which pneumatic transport would occur, this constitutes a large margin of error and rules out the possibility that the gas flows used were high enough to entrain bed material particles of the SMD in question.

Rather than the particles of a diameter close to the SMD for the entire particle population, it is more likely that the smaller particle sizes that was not be removed from the bed materials leaves the system since smaller particles are more easily entrained from the bed. But according to estimations based on calculation of U_t in steam, particle entrainment does not happen unless particles are as small as 40 µm even if the gas flows are doubled from the normal values. While the sand and olivine did not contain measurable amounts of particles below 75 µm, the bauxite had a 5 % content of these fines. Given that only a smaller fraction of these fines are of a diameter less than 40 µm, particle entrainment of raw bed materials is not considered to have occurred on any significant scale. However, it is possible that bed materials or char particles are subjected to a size reduction through mechanical abrasion, causing these particles to leave the bed. These effects are assumed to be similar across the experiments in the same set since conditions were similar, and therefore to not influence the results of the work. This

[5] Interpolated using 3rd degree polynomial of data series in Appendix C, page 332 of BASU, P. 2010. *Biomass gasification and pyrolysis: practical design and theory*, Academic press.

assumption is supported by the mass balance calculations presented in Appendix J, as no systematic difference between bed materials could be noted.

The reference experiment showed that no particle entrainment occurred on a large scale, where a maximum of 0.5 % of the bed material was entrained in the case of olivine. The sieve analysis indicated this might be an overstatement of particle entrainment as it was estimated that no more than 0.1 % of the bed material was of a size small enough to be entrained. If the particle entrainment was within the bounds as shown in the reference experiment, entrainment would have a small effect on the analysis results. Particle entrainment is therefore not considered a significant source of uncertainty for the conclusions.

Appendix G. Example logger data from a set *i* experiment

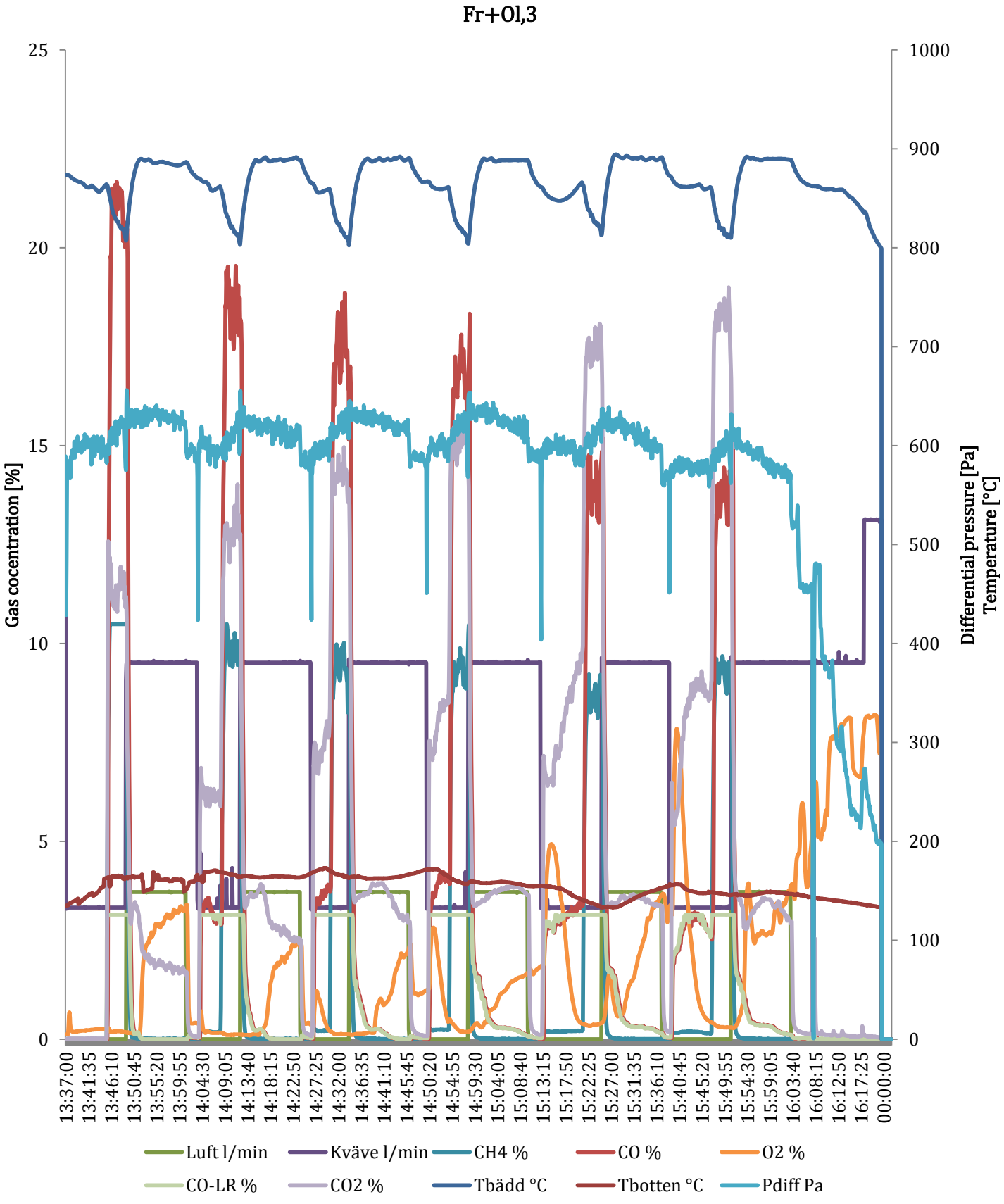

Appendix H. XRF analysis: set *i* experiments

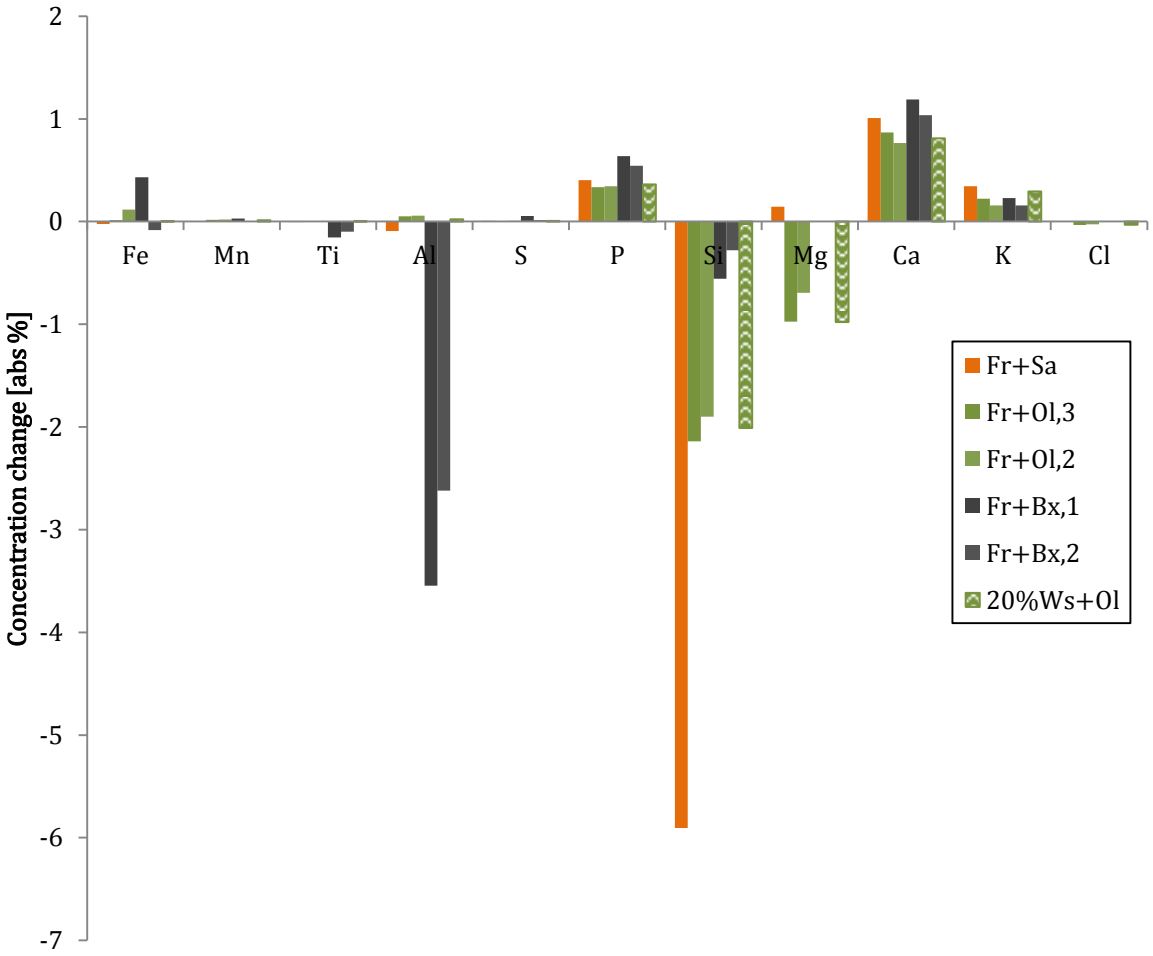

Appendix Figure H-1. XRF analysis result of the set *i* experiments expressed in terms of surface concentration change, including all elements.

Appendix I. Calibration details

Before conducting the first experiment the water pump and mass flow regulator used were calibrated. Calibration curves from these was used in order to correct the subsequent instrument settings throughout the experiment period.

Prior to every experiment, the gas measuring instruments were calibrated for zero and span values using calibration gases of known concentration or feeding appropriate flows of pure gases using the mass flow regulator. The measurement of CO was carried out on an instrument that was not span calibrated due to unavailability of a calibration gas of a sufficiently high concentration. The instrument did show correct readings for gases of 2.5 and 8 % CO, respectively. However, all CO readings above this concentration might be subject to error. As stated in Section 4.4, the methane instrument exceeded the 10 % range for all gas measurements of gas yield in, at least, the first cycle of all set *i* experiments. The values presented which give a value over 10 % are therefore to be regarded as estimations. These values, however, fit the general trends of the gas yield of methane in the calibrated ranges. In this context it should be noted that the absolute concentrations of the gases are not a core interest of this work, as the objective is to distinguish trends in gas concentrations. Even when regarding the potential systematic error in CH_4 and CO measurement due to calibration errors, this purpose is fulfilled.

Appendix J. Mass balance

If bed material particles are entrained out of the bed at a different rate for different bed materials, this would affect the mass balance and therefore the XRF measurements of element concentration giving rise to systematic errors. In the ideal case, no bed material particles would be entrained out of the bed during the course of the experiments and the mass of the samples taken should equal the mass of the virgin bed material plus the ash content of the added fuel. In order to evaluate this, all samples taken were weighed. From the total sample mass, the calculated addition of ash elements from the fuel was subtracted. The results are presented in Appendix Figure J-1.

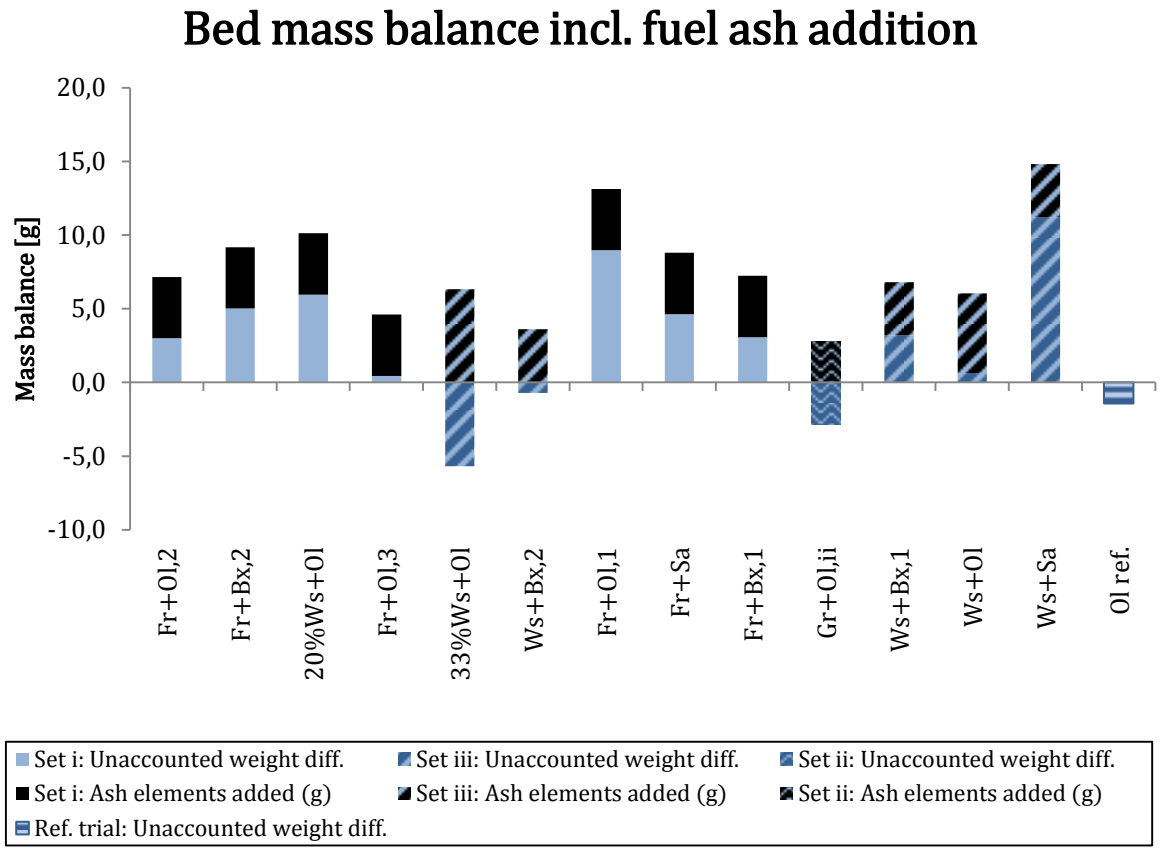

Appendix Figure J-1. Mass balance of all samples taken. Includes hot samples, residual samples and documented spillage

In Appendix Figure J-1, the unaccounted mass difference is defined as:

$$Unaccounted\ weight\ difference = Total\ sample\ mass - Calculated\ mass\ of\ ash\ added$$

The ash mass added is calculated based on the ash content of the fuel used. The fuel ash content was taken from the lab analysis data presented in Appendix C.

The sum of the black bars and the non-black bars corresponds to the total mass balance comparing the outputs (sample mass) to the inputs (virgin bed material and ash elements originating from fuel). The black bars represent the calculated addition of ash elements from fuel and is always positive. The non-black bars represent the mass balance unaccounted for: the change in mass that cannot be explained by ash addition. Positive non-black bars correspond to a mass gain over the course of the experiment, most likely originating from residual char that has not fully combusted. Negative non-black bars correspond to mass loss over the course of the experiment. Probable causes of mass loss are spillage in sampling and/or entrainment of fine particles. Note that the calculation assumes all ash elements are retained on the bed material, which is not the case.

In the majority of the experiments a positive mass balance was noted, most likely due to not fully combusted char remaining in the bed material. This gives rise to different mass concentration of all elements measured in the sample: uncombusted carbon dilutes the sample and affects the XRF analysis results, since these are expressed as mass concentration of elements. It is therefore desired to have a similar (and positive) mass balance for all experiments. However, the difference in mass balance comparing any two experiments, where samples were analyzed using XRF, is not above 20 grams. This should be weighed against the total mass of virgin bed material added: 300 g. Therefore, the difference in char content of the samples should not give rise to any larger uncertainties in comparing the XRF analysis results.

SLU
Institutionen för energi och teknik
Box 7032
750 07 UPPSALA
Tel. 018-67 10 00
pdf.fil: www.slu.se/energiochteknik

SLU
Department of Energy and Technology
P. O. Box 7032
SE-750 07 UPPSALA
SWEDEN
Phone +46 18 671000